

École Joliot-Curie 2015

“Instrumentation, detection and simulation in modern nuclear physics”

Nuclear Structure studies using *Advanced-Gamma-Tracking* techniques

Caterina Michelagnoli

michelagnoli@ganil.fr



In-beam γ -ray spectroscopy: requirements

Energy resolution ($E_\gamma \sim 10 \text{ keV} - 10 \text{ MeV}$),

in order to disentangle complex spectra

→ germanium detectors

Peak to Total ratio (large continuous Compton background),
in order to maximize “good events”

→ Compton background suppression

Doppler correction capability,

energy resolution dominated by Doppler broadening if the velocity vector and the emission angle of the γ -ray are not well known ($\beta \sim 5\text{-}10\%$, up to 50%)

Good solid angle coverage (ideally 4π), in order to maximize efficiency

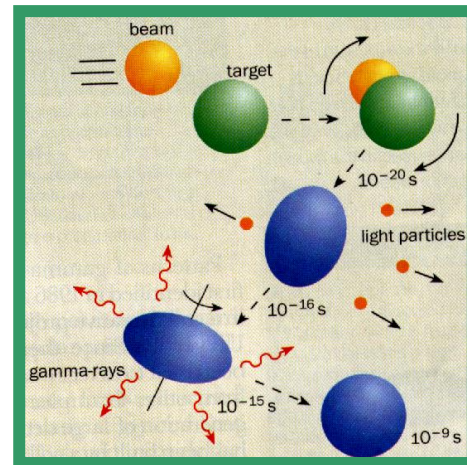
Good granularity ,

in order to reduce multiple hits on the detectors for high γ -ray multiplicity events

Avoid dead materials that could absorb radiation (→ preserve low energies)

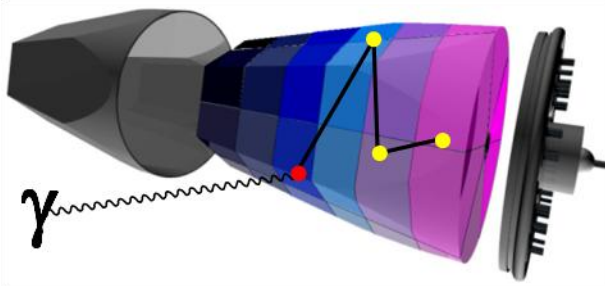
High counting rate capability (frequently background much stronger than channel of interest)

Time resolution (prompt events selection, lifetimes)



Position-sensitive operation mode and γ -ray tracking

highly segmented
HPGe detectors

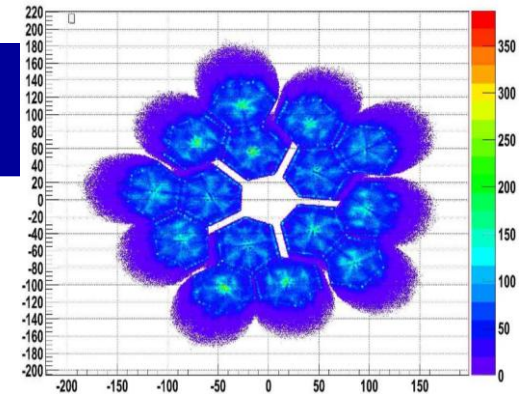
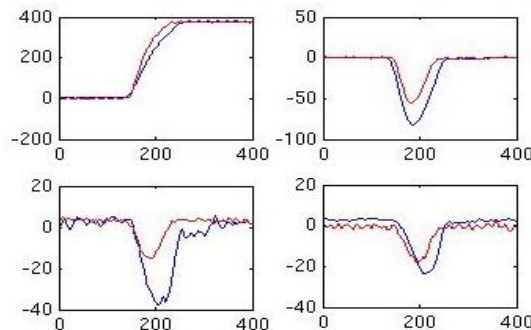


digital electronics to
record sampled
waveforms

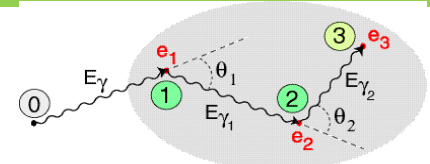
Identified
interaction points
(hits)

$(x, y, z, E, t)_i$

Pulse Shape Analysis
of the recorded waves



reconstruction of
 γ -rays from the hits
(tracking)



Event by event:
how many gammas,
for each gamma: energy,
first interaction point, path

Outline

PART 2 (September 29th 2015)

Pulse Shape Analysis (PSA)

1. Signal bases calculation
2. Signal decomposition

Some results from Ge position sensitive mode operation and γ -ray tracking

The AGATA array of segmented HPGe detectors

1. Implementation of Pulse Shape Analysis and Tracking concepts
2. The AGATA detectors and preamplifiers
3. The structure of electronics and data acquisition
4. Digital signal processing (at high counting rate)
5. (AGATA data processing)

AGATA+VAMOS (magnetic spectrometer) at GANIL

(be aware ... personal 😊selection of topics!)

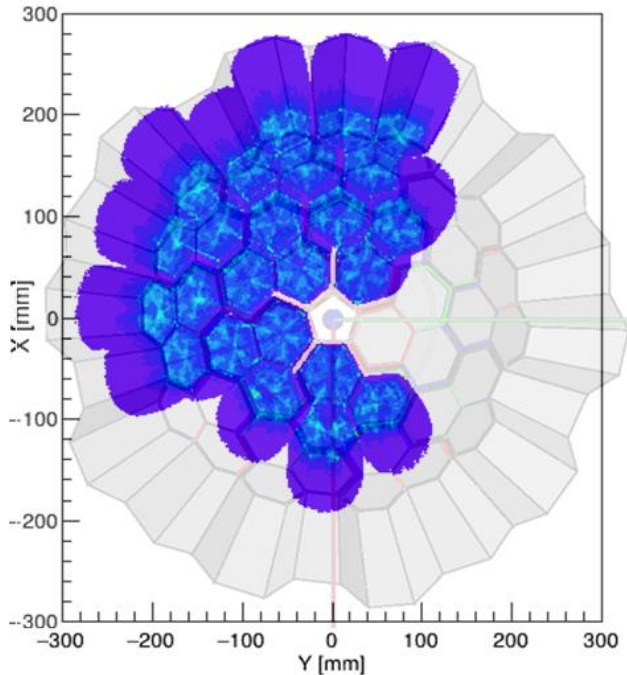
Pulse Shape Analysis (PSA)

comparison of net charge/transient signals
with reference signal basis

How do we build a basis of
reference signals ??

*Detector scanning (scanning tables):
practically unfeasible*

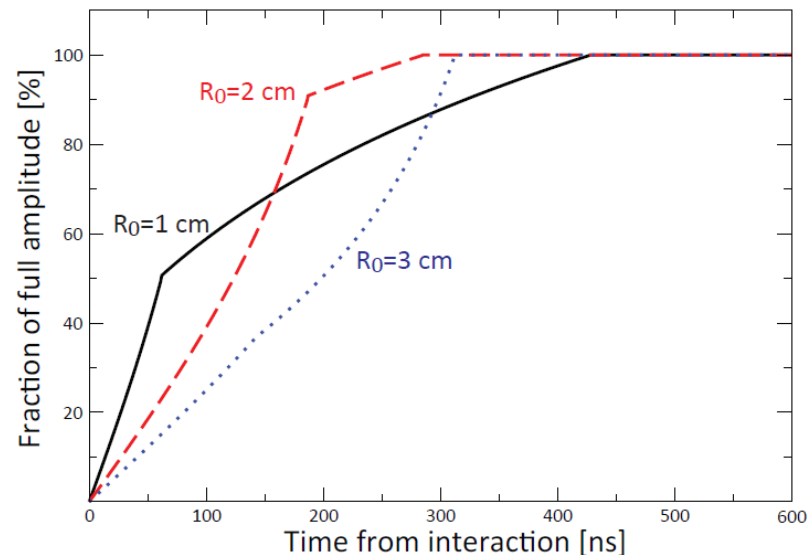
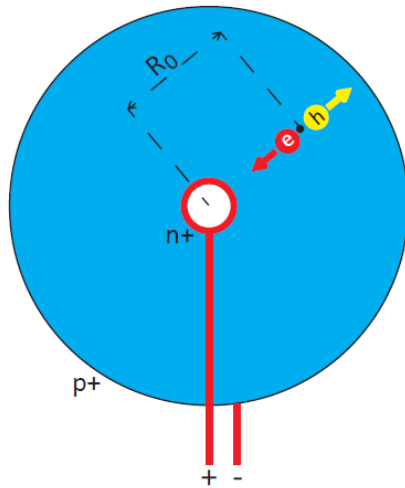
⇒ Signals Bases Calculations



Pulse shapes in a coaxial Ge detector

Reverse bias (-HV on p⁺ contact) depletes bulk and generates high electric field

Radiation → carriers in the bulk, swept out by electric field → signal



On “true” coaxial detectors, the shape depends on initial radius

Signal Formation

- Signal : motion of charge carriers (e/h) inside the detector volume;

$$\vec{v}_{e/h} = \mu_{e/h} \vec{E} \quad (\mu_{e/h} = \text{electron/hole mobility})$$

- Calculation of charge induced in an electrode due to motion of charge carriers in a detector: Ramo Theorem and concept of weighting potential

$$i(t) = q \vec{v} \cdot \vec{E}_W \quad E_W = \text{weighting field}$$

$$Q = q \Delta\varphi_W \quad \varphi_W = \text{weighting potential}$$

$\varphi_W = \varphi_W(\vec{x})$ solution of the Laplace equation (for given detector geometry)

with voltage of the electrode for which induced charge is calculated = 1 and other electrodes at zero

Signal Formation

- Signal : motion of charge carriers (e/h) inside the detector volume;

$$\vec{v}_{e/h} = \mu_{e/h} \vec{E} \quad (\mu_{e/h} = \text{electron/hole mobility})$$

- Calculation of charge induced in an electrode due to motion of charge carriers in a detector: Ramo Theorem and concept of weighting potential

$$i(t) = q \vec{v} \cdot \vec{E}_W \quad E_W = \text{weighting field}$$

$$Q = q \Delta\varphi_W \quad \varphi_W = \text{weighting potential}$$

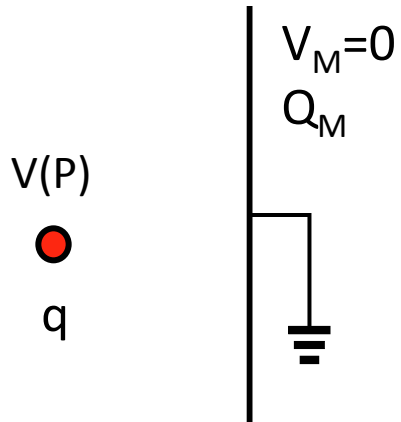
$\varphi_W = \varphi_W(\vec{x})$ solution of the Laplace equation (for given detector geometry) with voltage of the electrode for which induced charge is calculated = 1 and other electrodes at zero

The Ramo theorem is based on the Green's reciprocity theorem

$$\sum_i V_i' Q_i = \sum_i V_i Q_i'$$

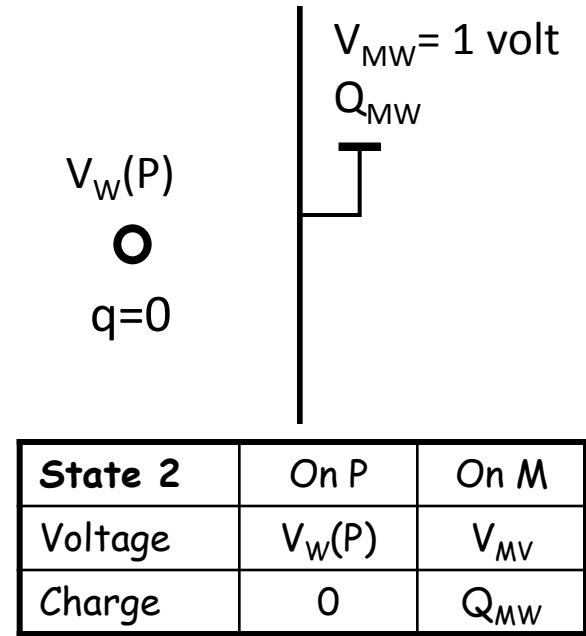
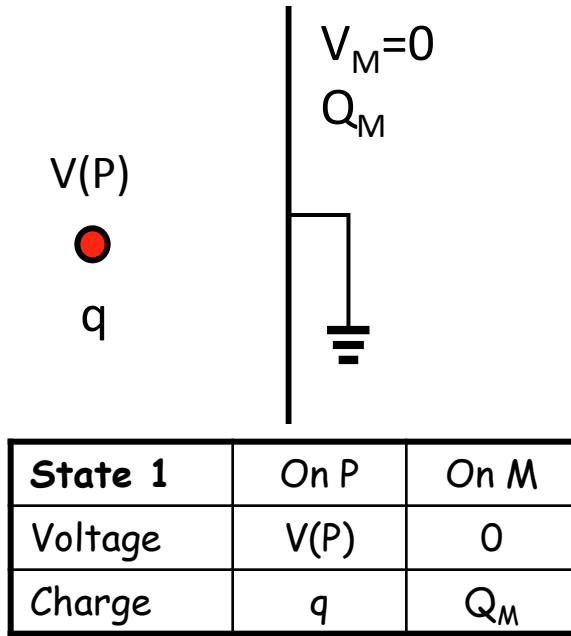
relation between two systems consisting of a distribution of charges and electrodes

Induced Charge

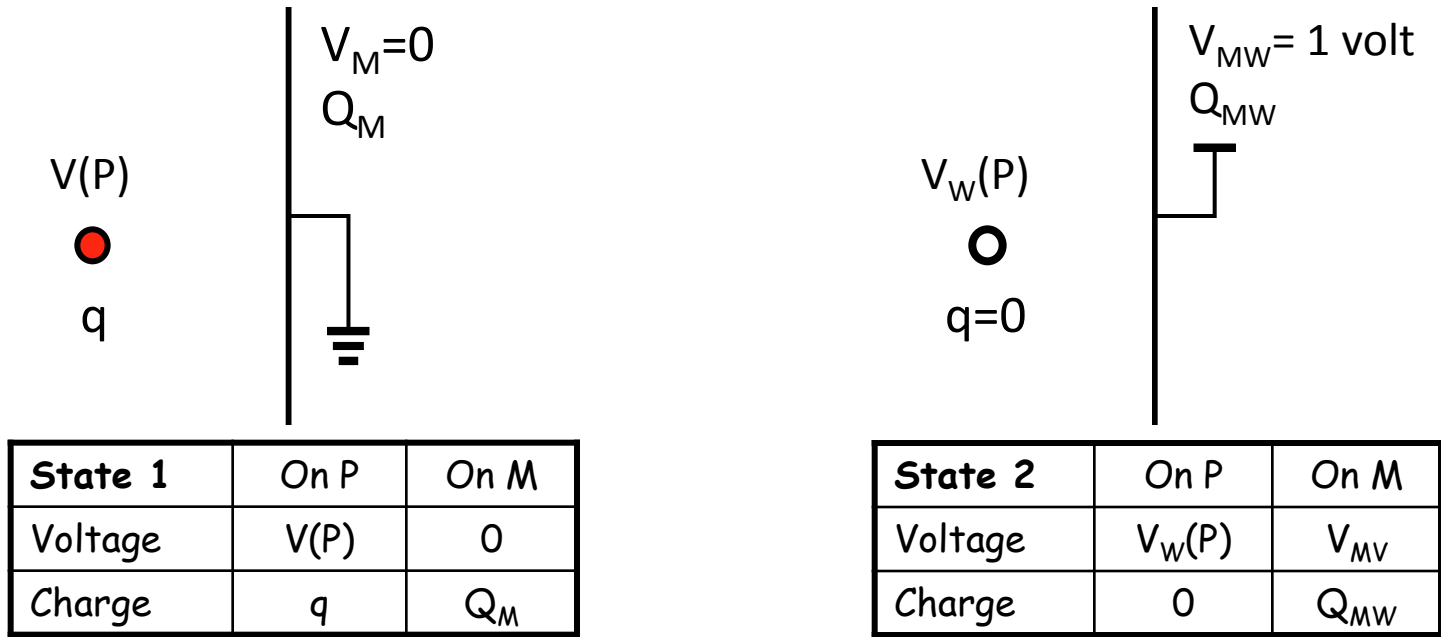


State 1	On P	On M
Voltage	$V(P)$	0
Charge	q	Q_M

Induced Charge



Induced Charge

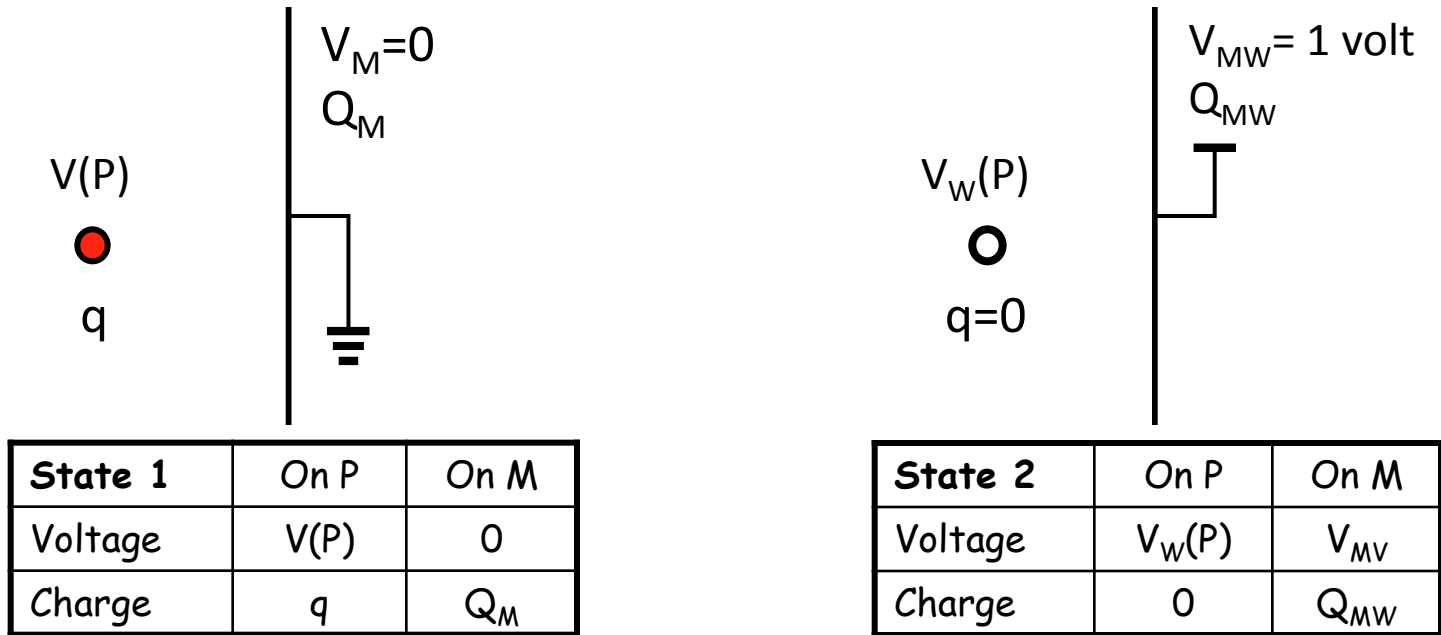


$$V(P) \cdot 0 + 0 \cdot Q_{MW} = q \cdot V_W(P) + Q_M \cdot V_{MW}$$

$$Q_M = -qV_W(P)$$

V_W dimensionless

Induced Charge



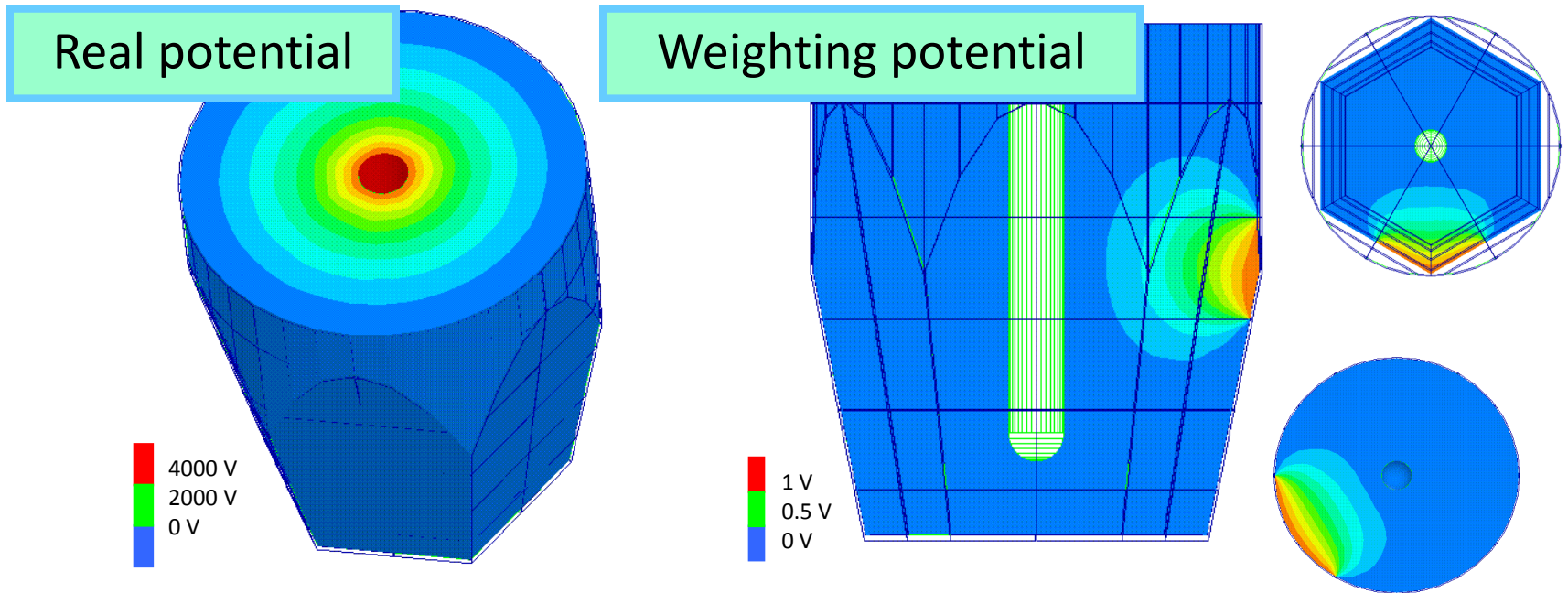
$$V(P) \cdot 0 + 0 \cdot Q_{MW} = q \cdot V_W(P) + Q_M \cdot V_{MW}$$

$$Q_M = -qV_W(P) \quad V_W \text{ dimensionless}$$

The charge induced in one of an electrode of the system by the charge q is given by the product of the inducing charge times the potential generated at the position of the charge when the charge itself is removed, the electrode of interest (sensing) is put at $V = 1$ volt and all other electrodes of the system are put to ground.

Weighting potential

electrostatic coupling between the moving charge and the sensing electrode



Calculation of pulse shapes for real detectors

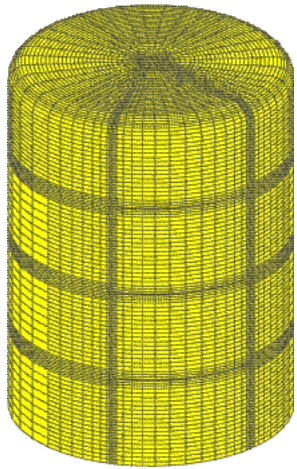
- Analytical solutions only for true coaxial
- Take a FEM modeler (your own, MAXWELL-3D, FEMLAB, ...)
 - Specify geometry, and segmentation
 - Specify material, impurity concentration and distribution
- Solve Poisson equation and get electric potential
- Use mobility of e/h to calculate trajectories
- Solve Laplace equation for all electrodes and get V_w
- Calculate induced currents / induced charge

Calculation of pulse shapes for real detectors

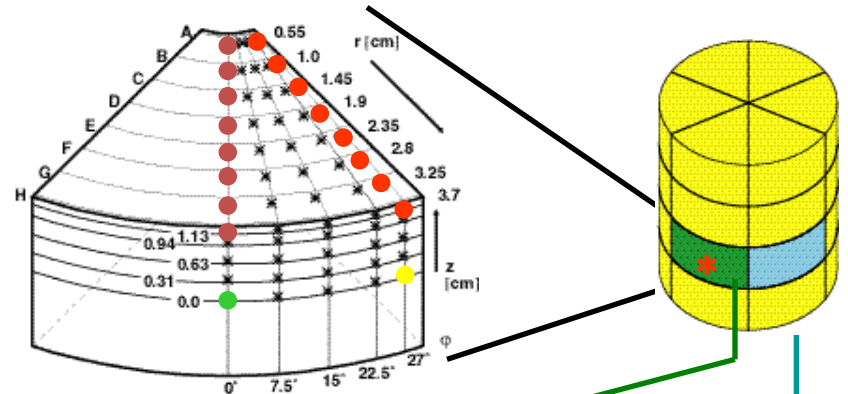
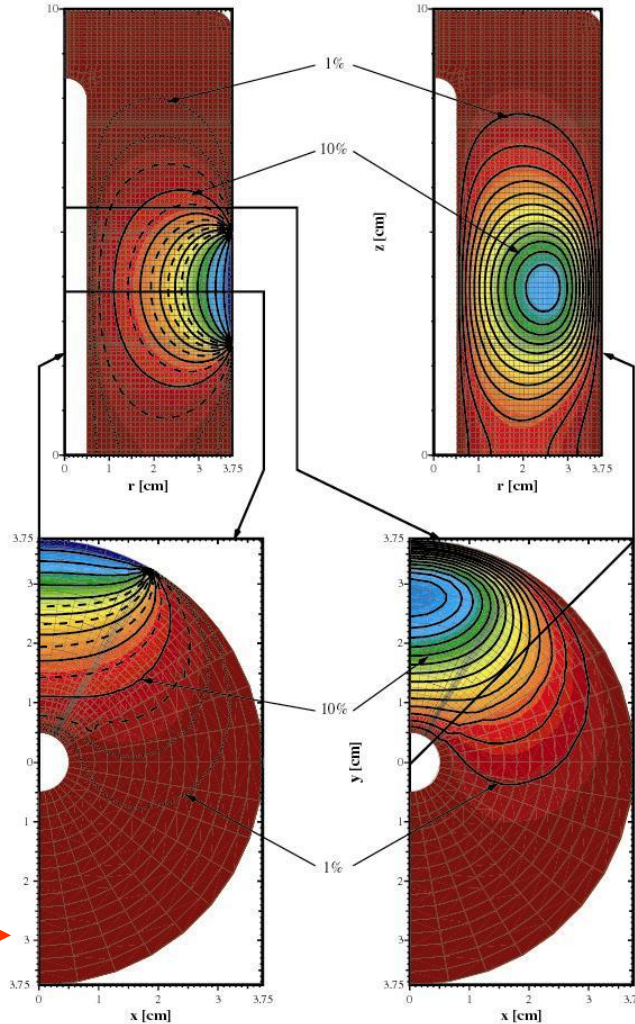
Calculation of the signals induced on the contacts using the **weighting field method**

$$i_{e/h} = -q_{e/h} \cdot \vec{E}_W \cdot \vec{v}_{drift} \left(\vec{E} \right)$$

FEM-model of detector

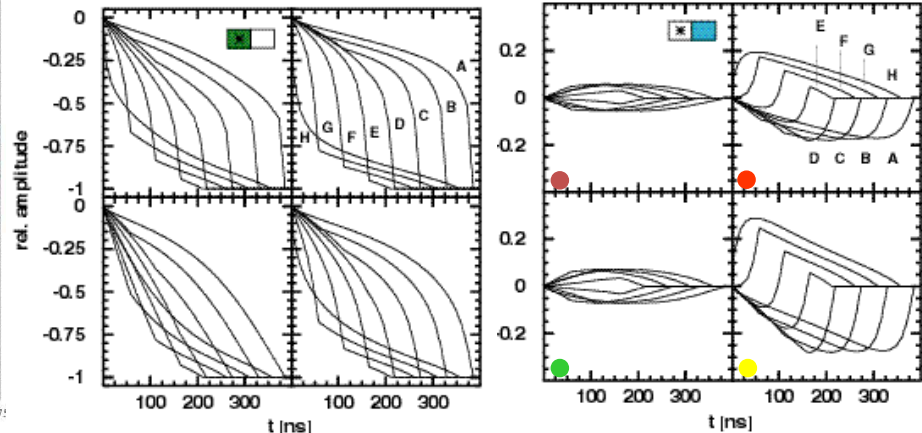


Calculate weighting fields



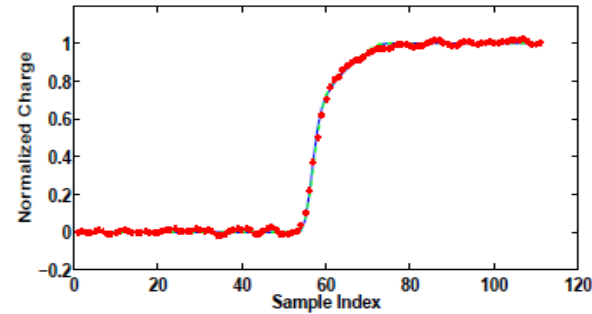
net charge signals

transient signals



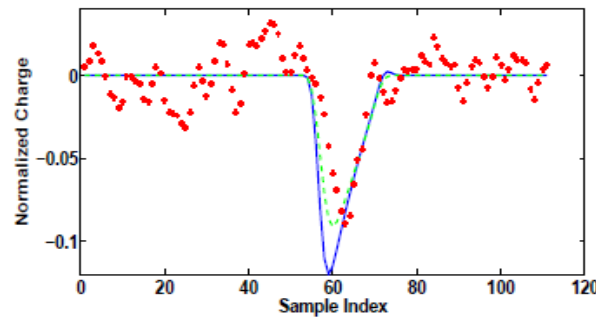
Simulated Signals

Signals after folding with the preamplifier response function and the analog filter functions (some smearing)
Full signal for each point in the detector.

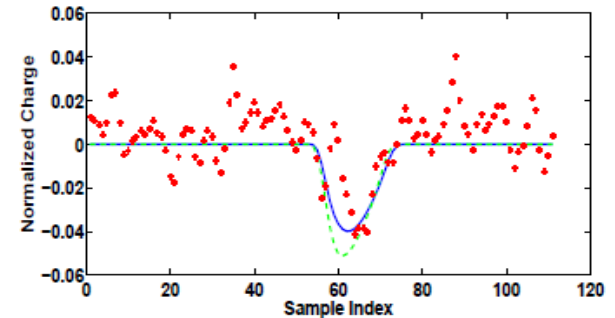


(a) Net charge signal in segment A4

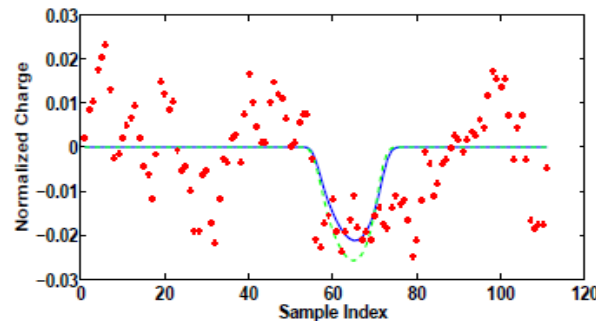
- experiment
- Set A
- - Set B



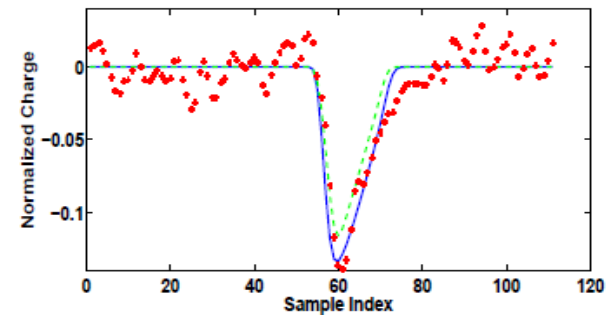
(b) Transient signal in segment A5.



(c) Transient signal in segment A3.



(d) Transient signal in segment B4.



(e) Transient signal in segment F4.

Parameters from experiment

Signal Decomposition or Pulse Shape Analysis (PSA)

Expand measured signals in terms of base signals
and determine expansion coefficients

$$S^{exp} = \sum_{i=1}^N A_i S_i^{base}$$

- Sampling every 10 ns, ~100 samples per involved segment
- Each base-point has 1 segment with net charge and 8-11 neighbours with transient signals
- With a grid of 1 mm a typical crystal has ~ 400000 base points (up to possible symmetries)

→ That's too much for a direct decomposition !!! ←

➡ Grid Search Algorithm

Verifying quality of Pulse Shape Analysis

- From simulations and calculations
 - **Generate** interaction points by MC simulation
 - **Calculate** pulse shapes (adding noise)
 - **Decompose** pulses into interaction points
- From experimental data with defined position
 - Scanning tables and coincidence methods with well collimated, strong radioactive sources can provide $\sim\text{mm}^3$ precision
- From experimental data: distribution of interaction points
- In-beam experiments with fast moving nuclei
 - Doppler shift correction depends on determination of gamma-emission angle, which depends on position of first interaction point

Complications for PSA

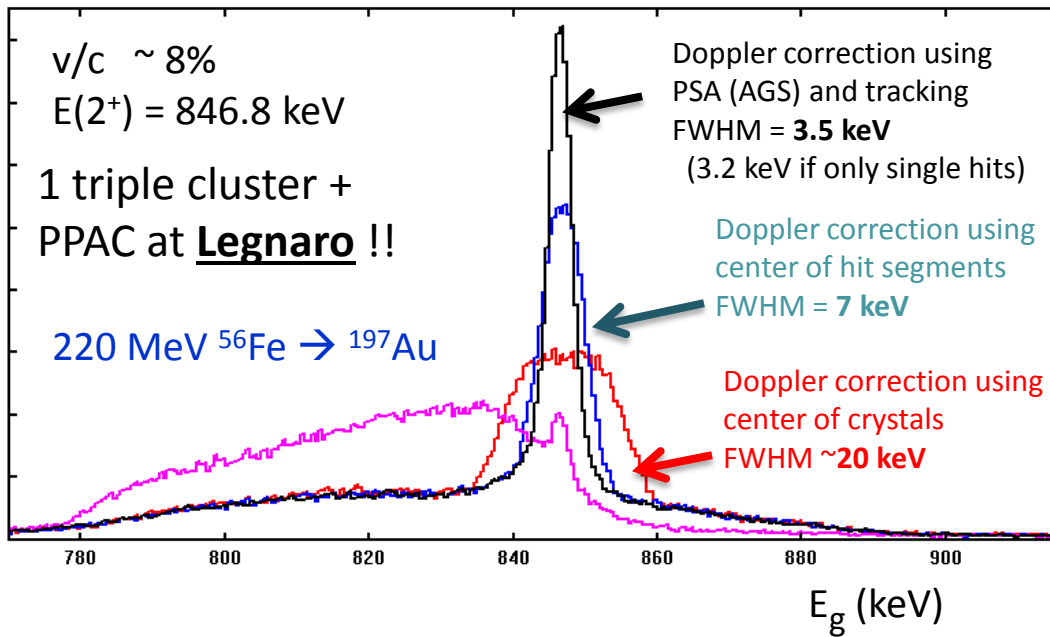
- No good theory for mobility for holes
- Mobility of charge carriers depend on collection path with respect to crystal lattice
- Detector irregular geometry (→ difficult bases calculation)
- Effective segmentation (electric field) \neq geometrical segmentation
- Position sensitivity not uniform throughout the crystal
- Computationally “heavy”
- Events with multiple hits per segment are difficult to analyze
- Low energy releases can end up far away from actual position

Performance of PSA

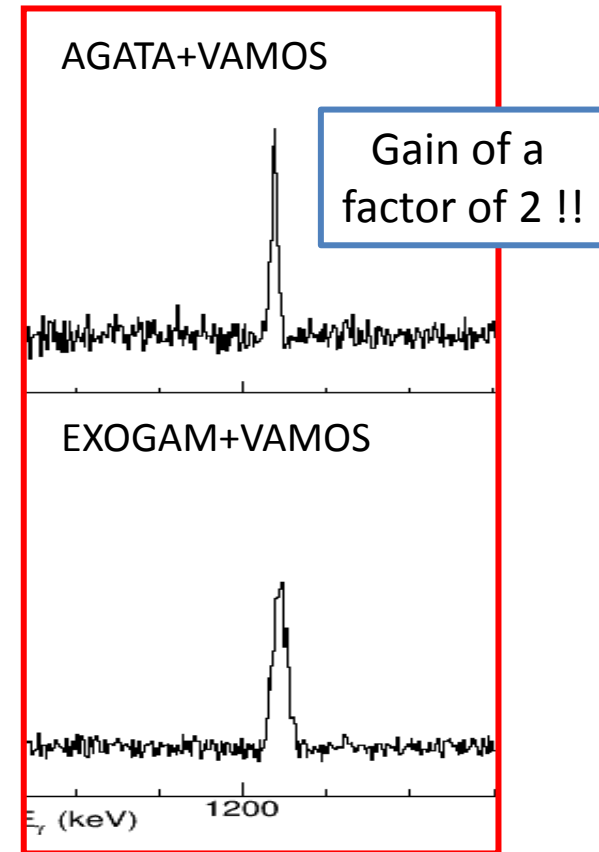
- Depends on the signal decomposition algorithm but of equal or more importance are:
- The quality of the signal basis
 - Physics of the detector
 - Impurity profile
 - Application of the detector response function to the calculated signals
- The preparation of the data
 - Energy calibration
 - Cross-talk correction (applied to the signals or to the basis!)
 - Time alignment of traces
- A well working decomposition has additional benefits, e.g.
 - Correction of energy losses due to neutron damage

Some benefits from position resolution
and γ -ray tracking

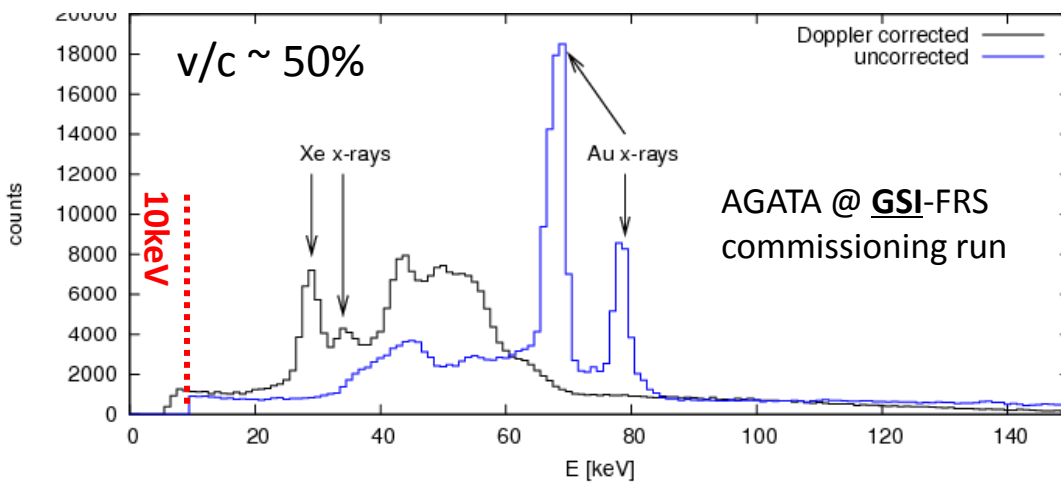
Doppler broadening: towards the intrinsic resolution in-beam



$2^+ \rightarrow 0^+ \quad ^{98}\text{Zr}$
 populated by fission
 GANIL

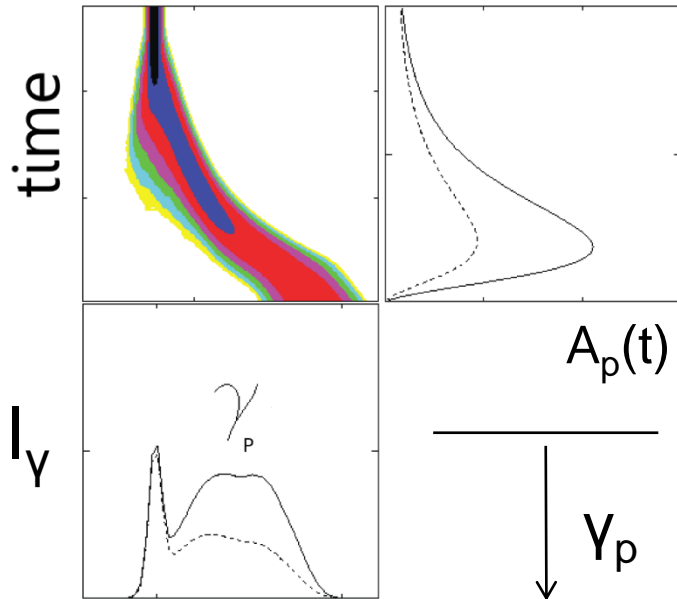
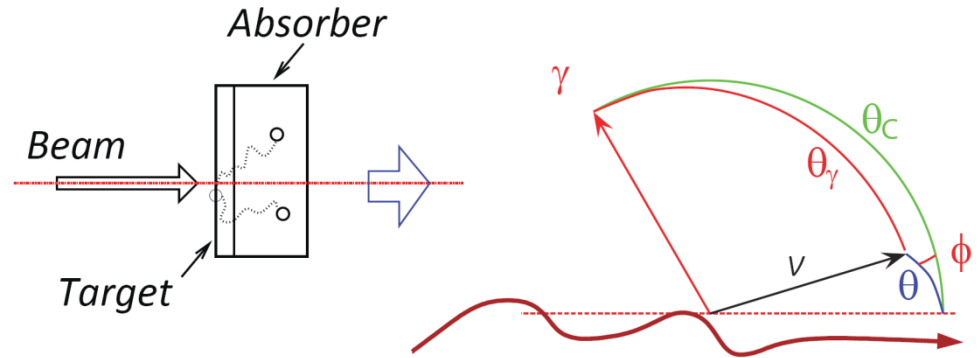


$^{136}\text{Xe} (137 \text{ MeV/u}) + ^{197}\text{Au}$



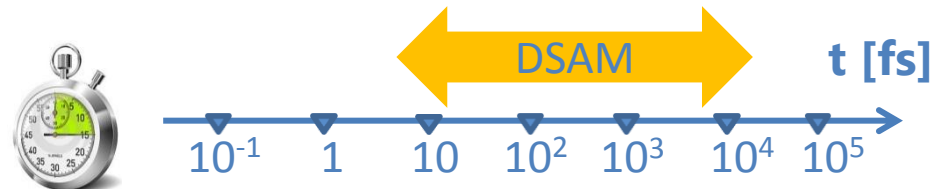
Doppler Shift Attenuation (DSA) for the measurement of nuclear level lifetimes

The lifetime of the excited state is compared with the slowing down time of the emitting nucleus in the absorbing material



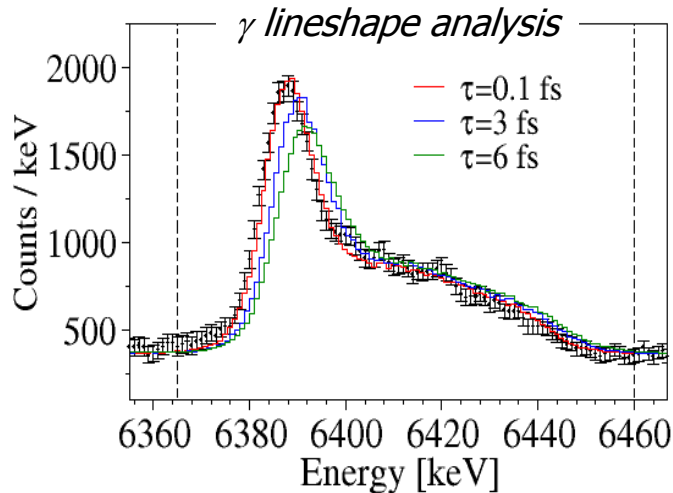
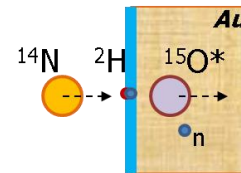
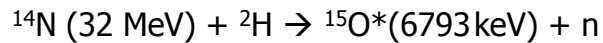
$$\overline{E_\gamma} = E_\gamma \frac{\sqrt{1 - \beta^2}}{1 - \beta \cos\theta} \quad \beta = \left| \frac{\vec{v}}{c} \right|$$

Monte Carlo simulations => lineshape analysis of the peaks observed in the γ spectrum



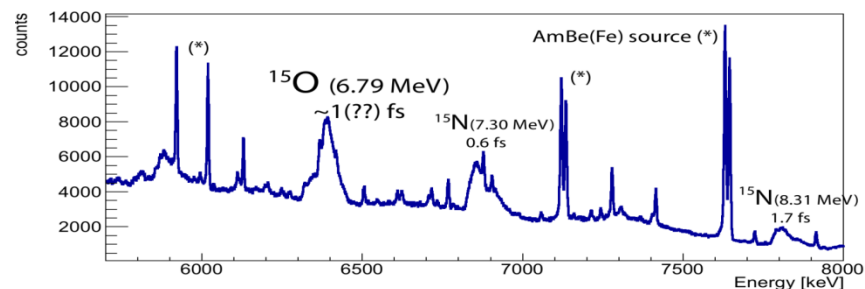
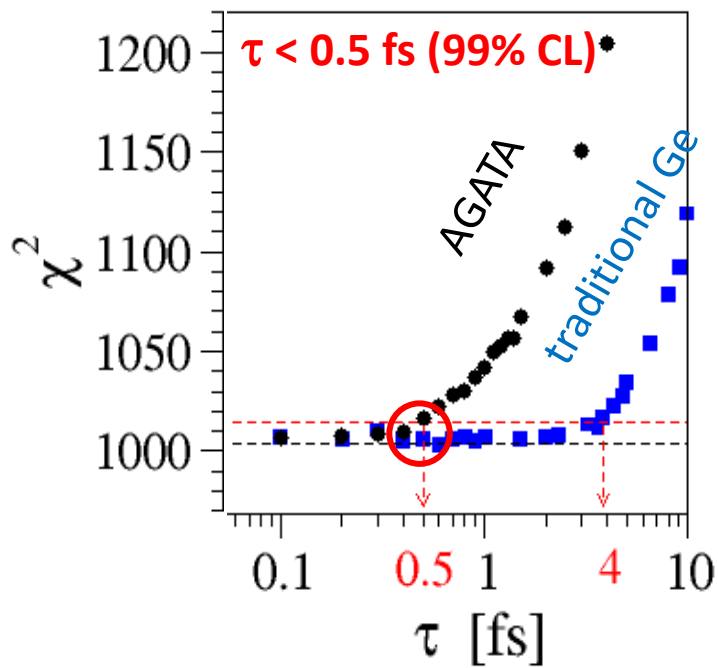
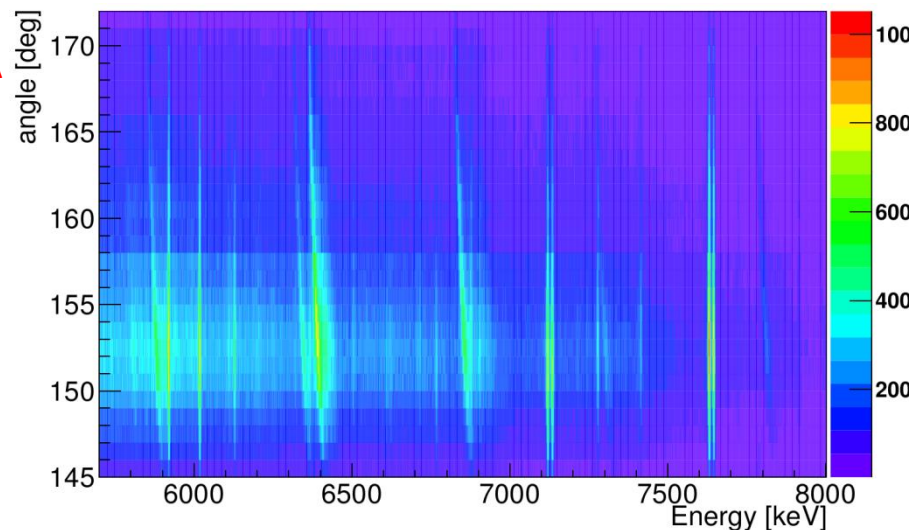
Sub-femtosecond lifetime measurements

AGATA Demonstrator at LNL



4 mm AGATA
position
resolution

2 degree
"θ slices"

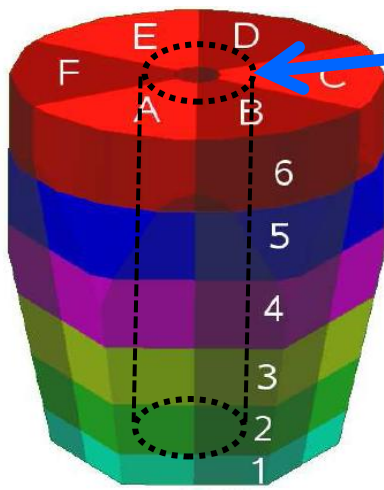
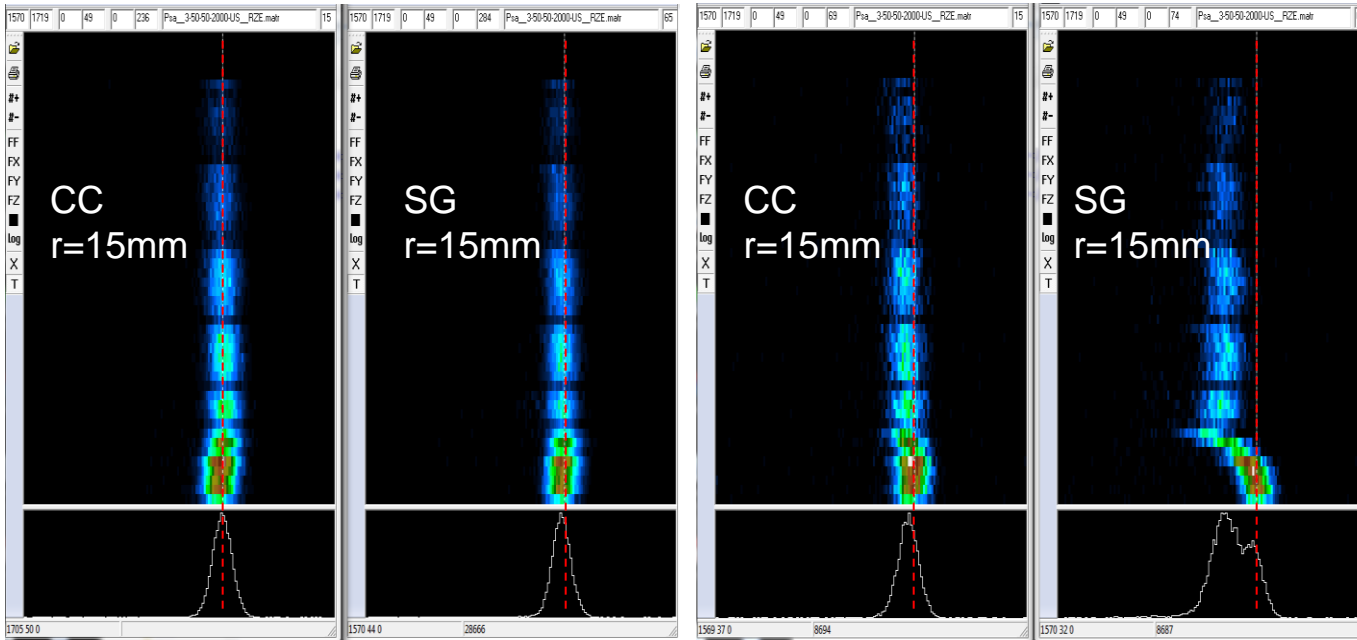


Doppler Shift Attenuation lifetime
measurements by lineshape analysis over
a continuous angular distribution

Neutron-damage correction

April 2010

July 2010



The 1332 keV peak as a function of crystal depth (z) for interactions at $r = 15\text{mm}$

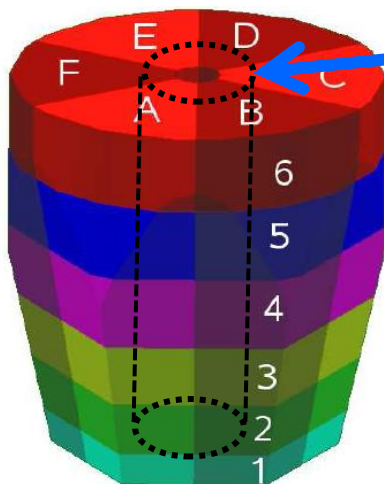
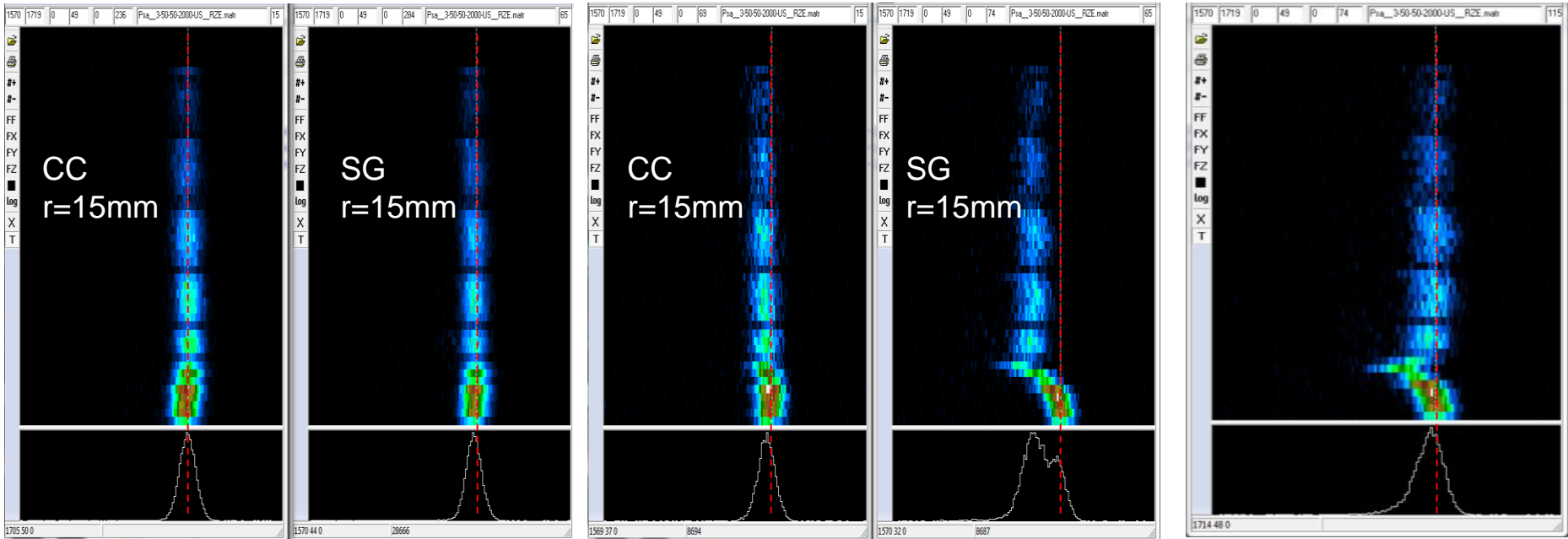
Charge loss due to neutron damage \rightarrow
proportional to the path length to the electrodes

Neutron-damage correction

April 2010

July 2010

→ corrected

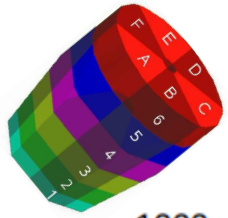


The 1332 keV peak as a function of crystal depth (z) for interactions at $r = 15\text{mm}$

Charge loss due to neutron damage → proportional to the path length to the electrodes

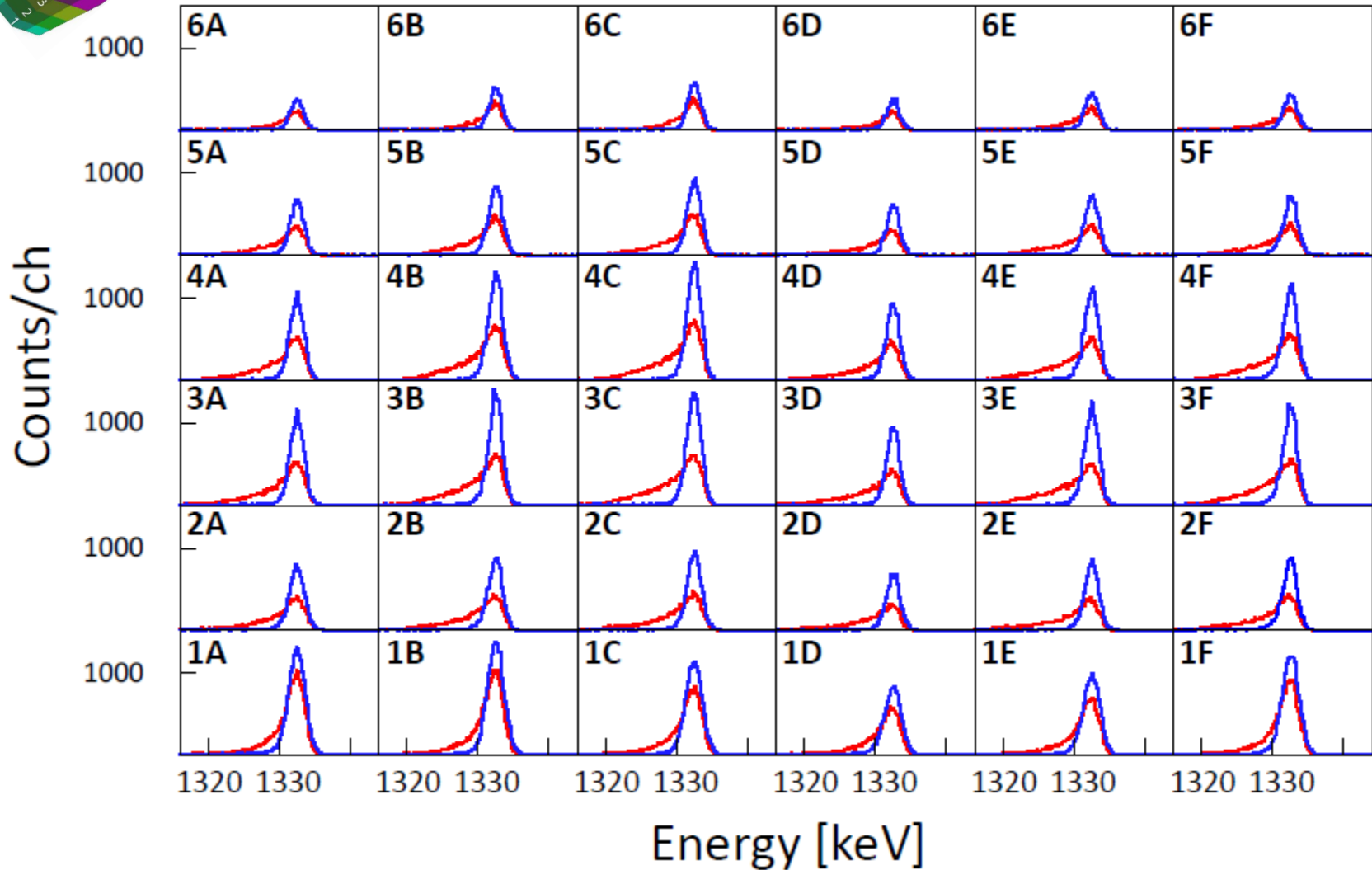
Use PSA interaction points and modeling of charge trapping to correct the effect

Effect of the correction on energy resolution



— corrected
— uncorrected

Sum of segments: 5.9 keV → 2.9 keV



The Advanced-Gamma-Tracking-Array AGATA

S. Akkoyun et al. NIM A 668 (2012) 26

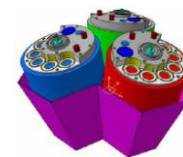
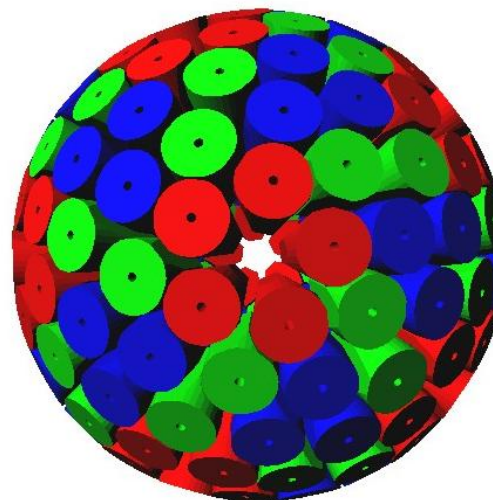
AGATA

(Advanced-GAMMA-Tracking-Array)



the “ γ -ray spectroscopy dream”

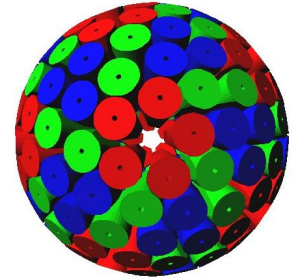
- High efficiency.
- Good position resolution on the individual γ interactions.
- Capability to stand a high counting rate.
- High granularity.
- Capability to measure the Compton scattering angles of the γ -rays within the detectors.
- Coupling to ancillary devices for added selectivity.



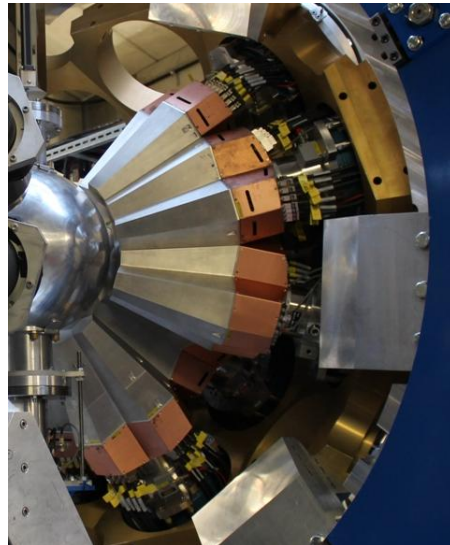
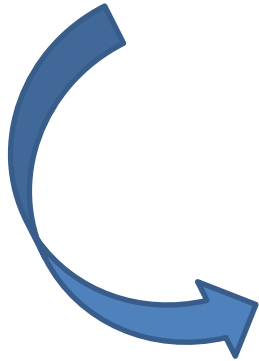
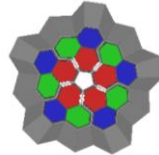
180 hexagonal crystals	3 shapes
60 triple clusters	all equal
inner radius	24 cm
amount of germanium	374 kg
solid angle coverage	79 %
6480 segments	
efficiency at 1MeV:	39% ($M_g=1$),
	25% ($M_g=30$)
Peak/Total:	53% ($M_g=1$),
	46% ($M_g=30$)

Geant4 Montecarlo simulations
E. Farnea, NIMA 621 (2010) 331

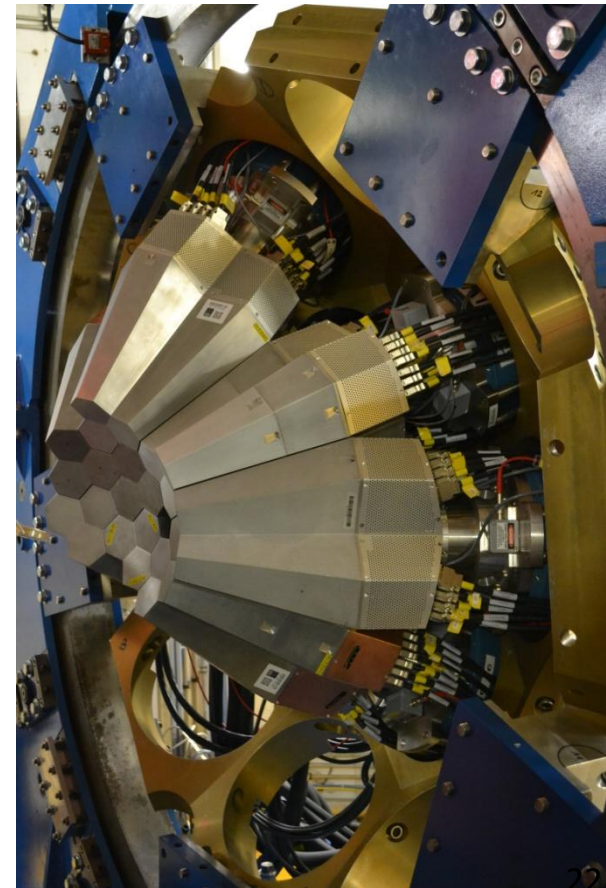
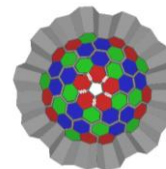
realization of the dream: AGATA the *nomadic detector*



Demonstrator at the Legnaro National Lab., Italy 2009-2012

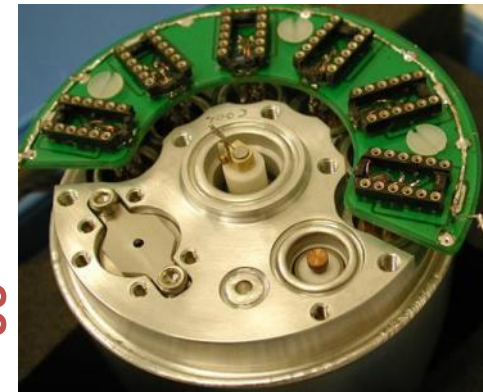
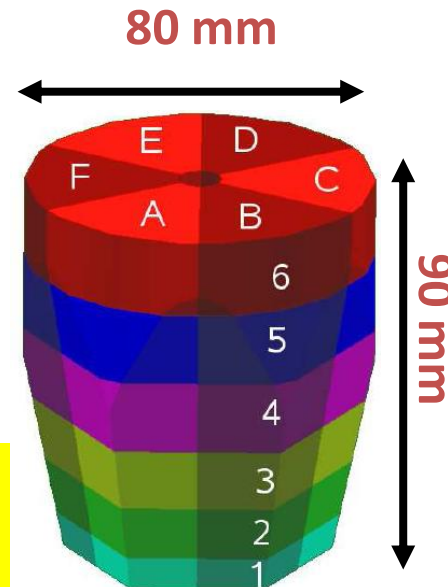
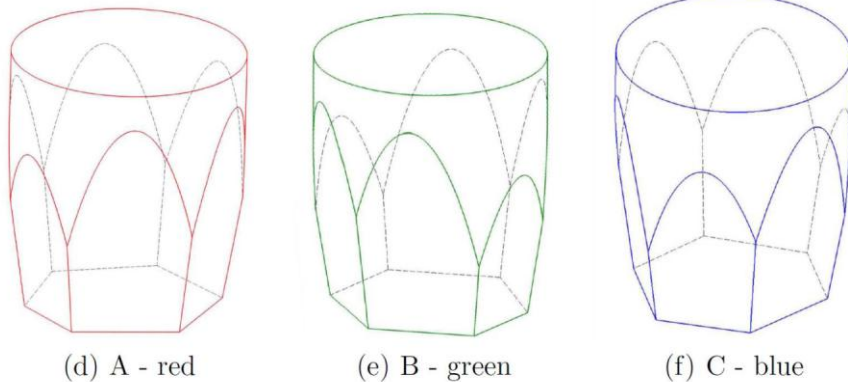
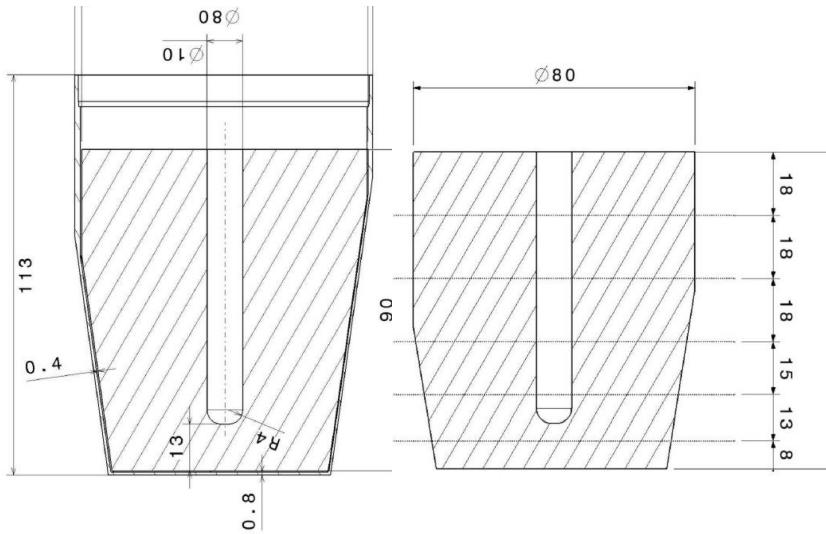


today AGATA is at GANIL, 2014-2018 France



*AGATA @ GSI
Germany
2012-2014*

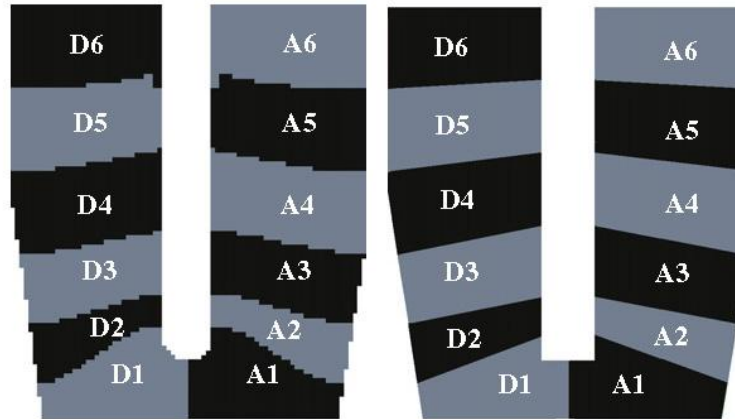
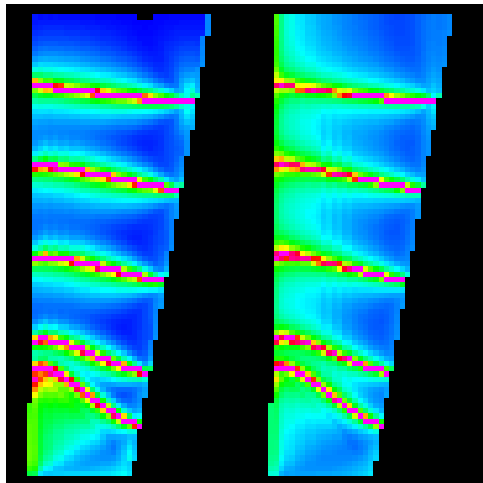
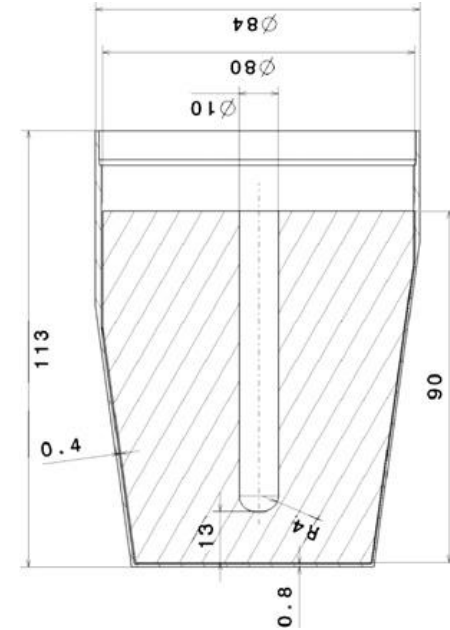
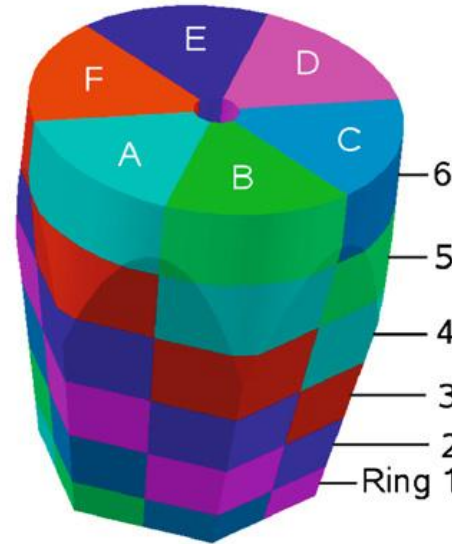
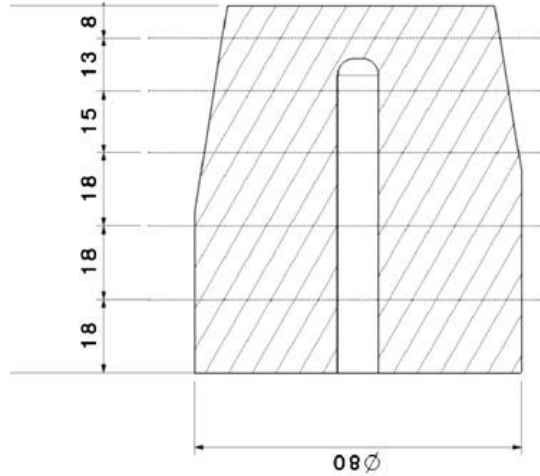
AGATA Crystals



Volume ~370 cc Weight ~2 kg
(the 3 shapes are volume-equalized to 1%)

6x6 segmented cathode

Segmentation of the AGATA detector



Implementation in GEANT4

Signals:
2 central contact
36 segments

Pulse Shape Simulations
Th. Kröll, A. Görden

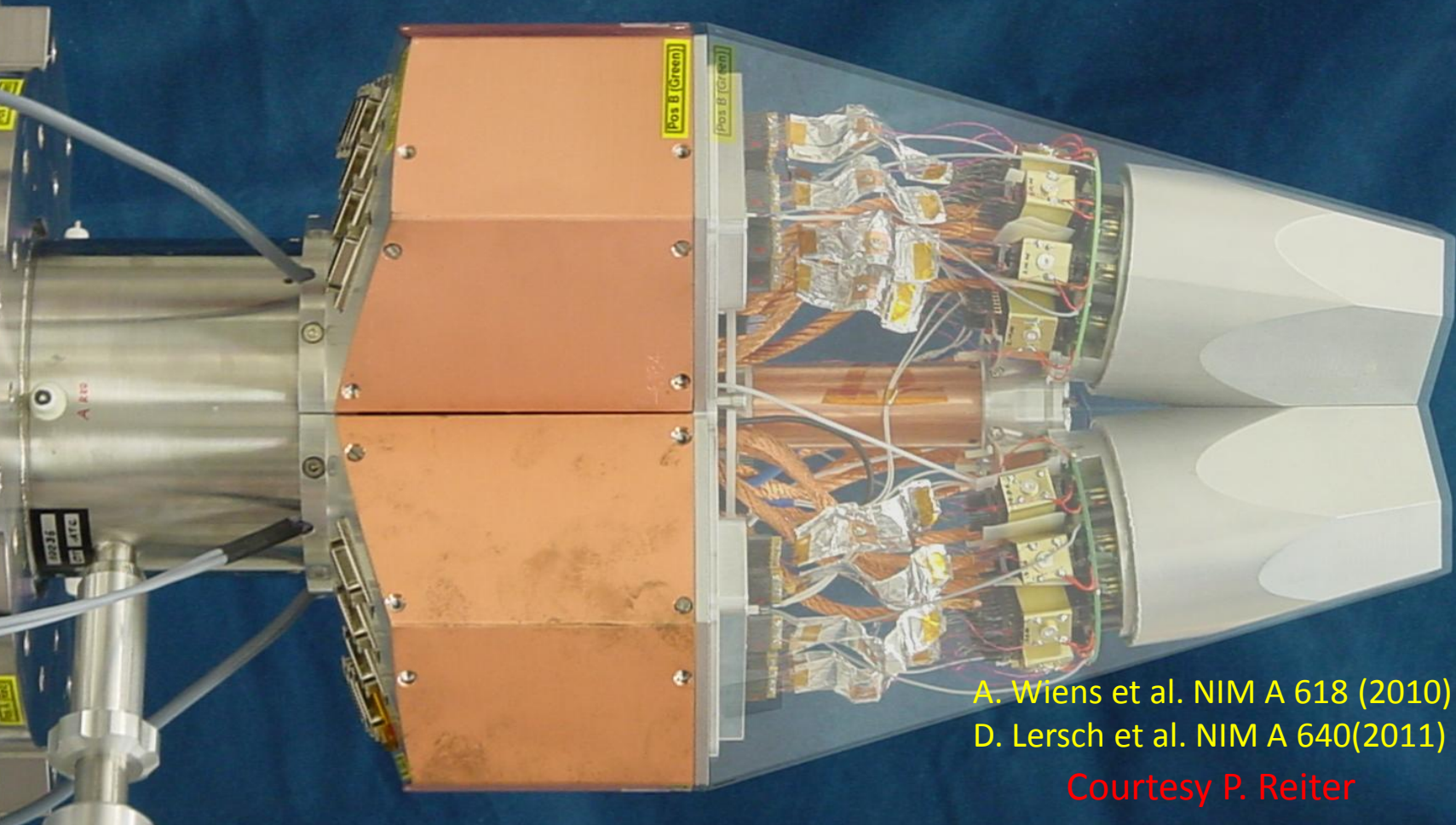
A.Wiens et al. NIMA 618 (2010) 223
E.Farnea et al. NIMA 621 (2010)331

Asymmetric AGATA Triple Cryostat

- integration of 111 high resolution spectroscopy channels
- cold FET technology for all signals

Challenges:

- mechanical precision
- heat development, LN2 consumption
- microphonics
- noise, high frequencies

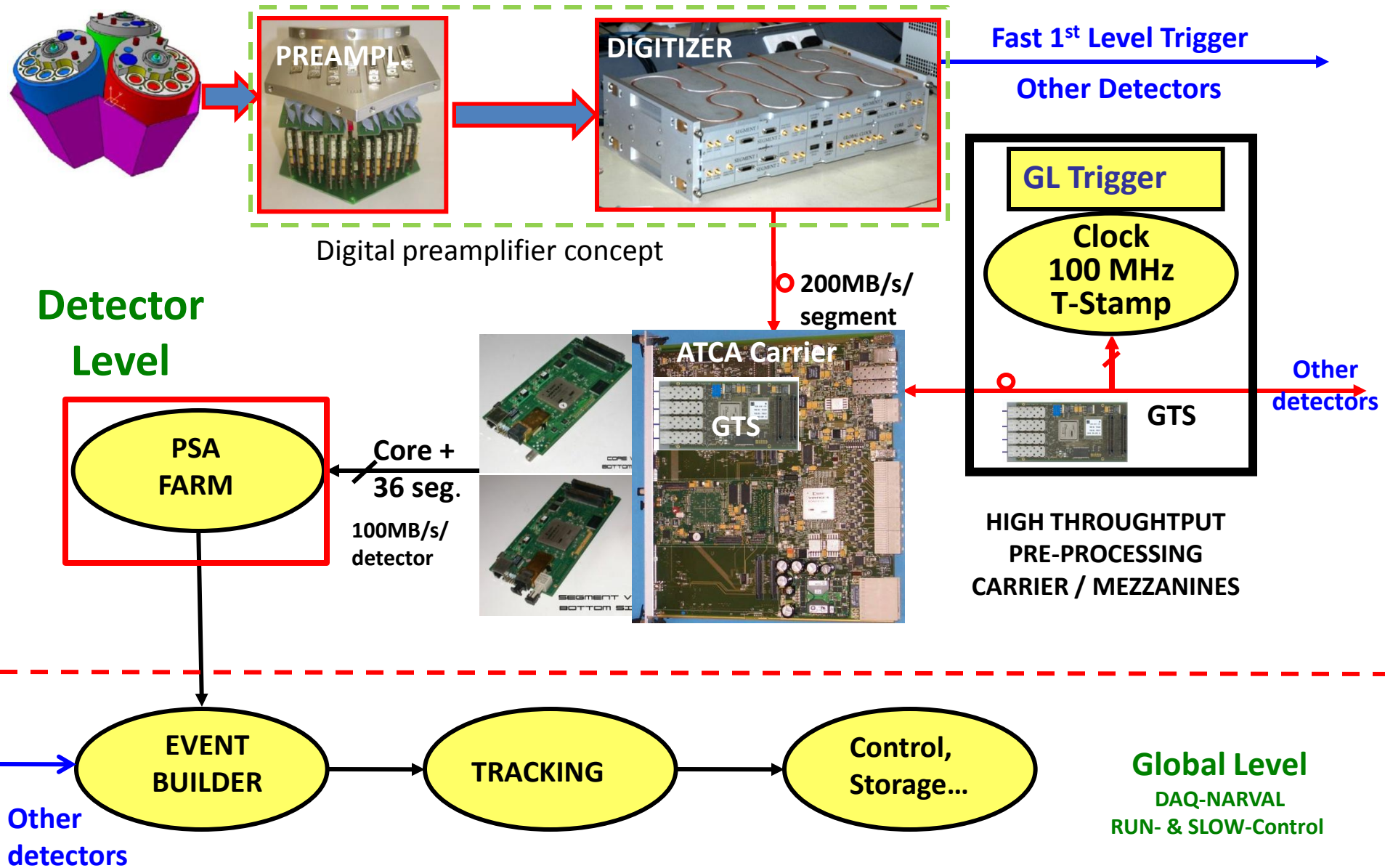


A. Wiens et al. NIM A 618 (2010) 223–233

D. Lersch et al. NIM A 640(2011) 133-138

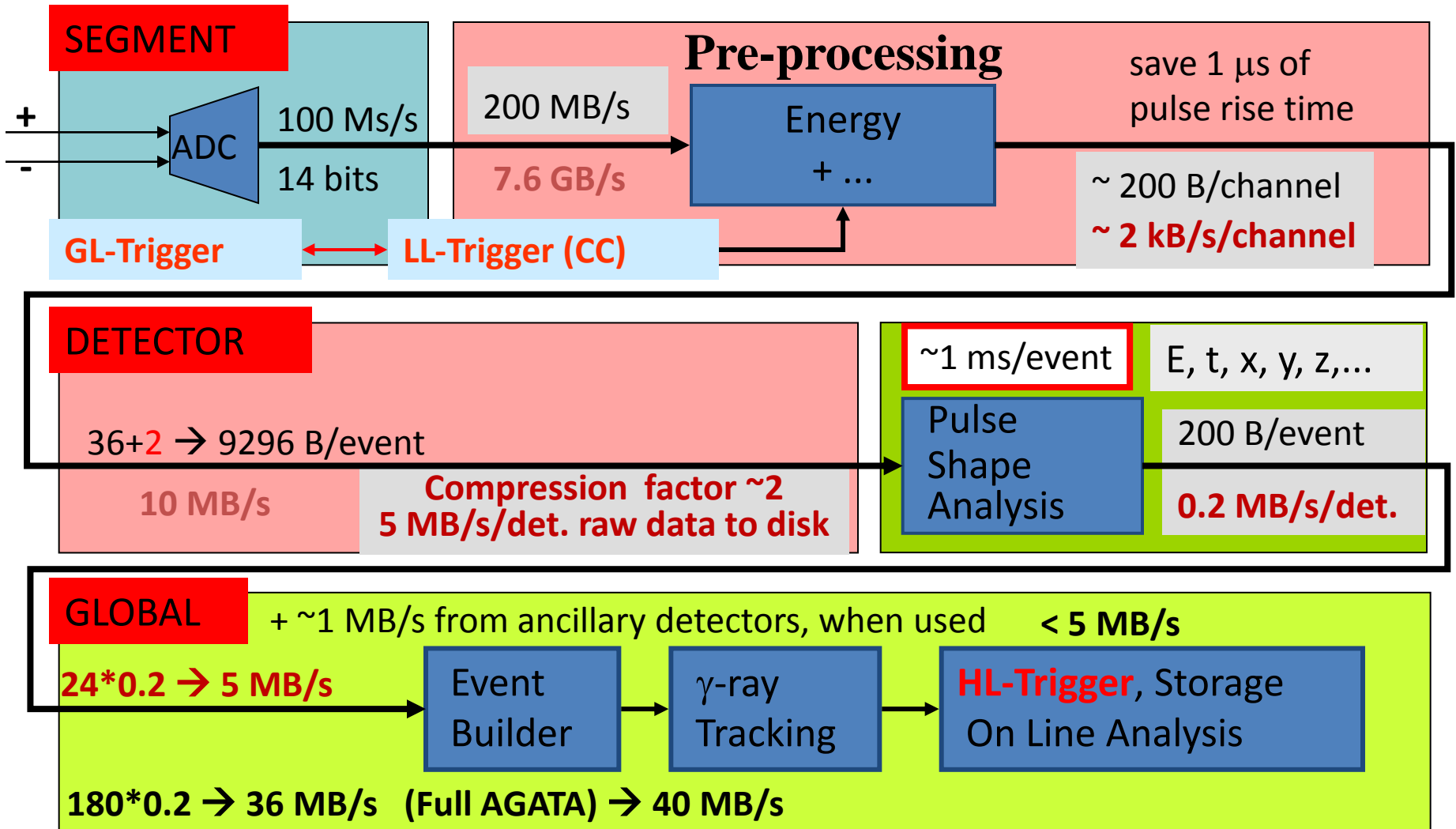
Courtesy P. Reiter

Structure of Electronics and DAQ



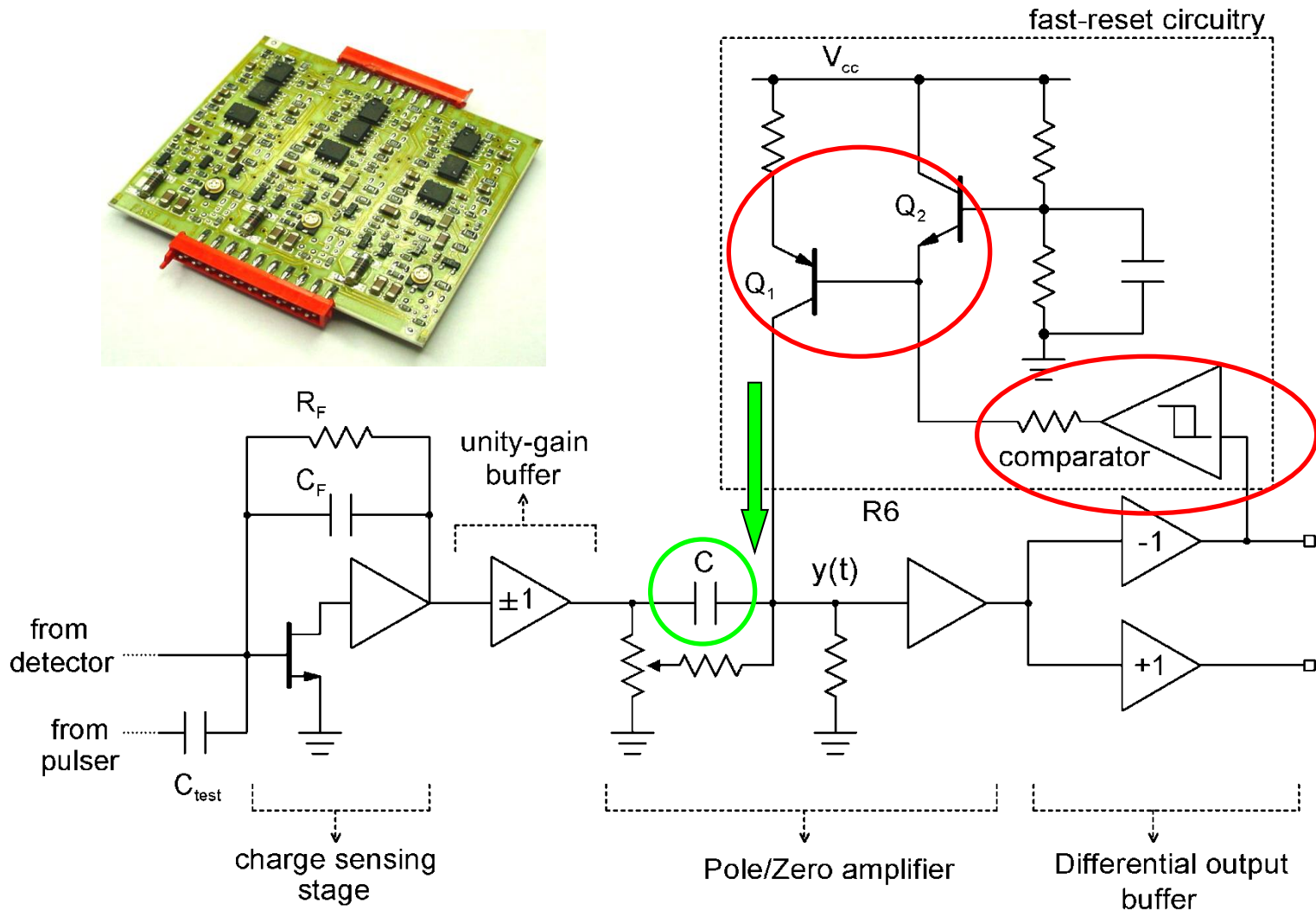
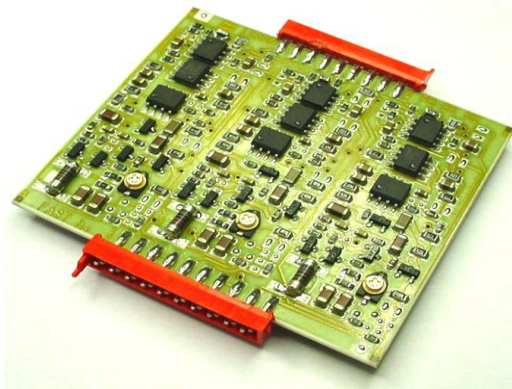
interface to GTS, merge time-stamped data into event builder, prompt local trigger from digitisers

Data rates in AGATA

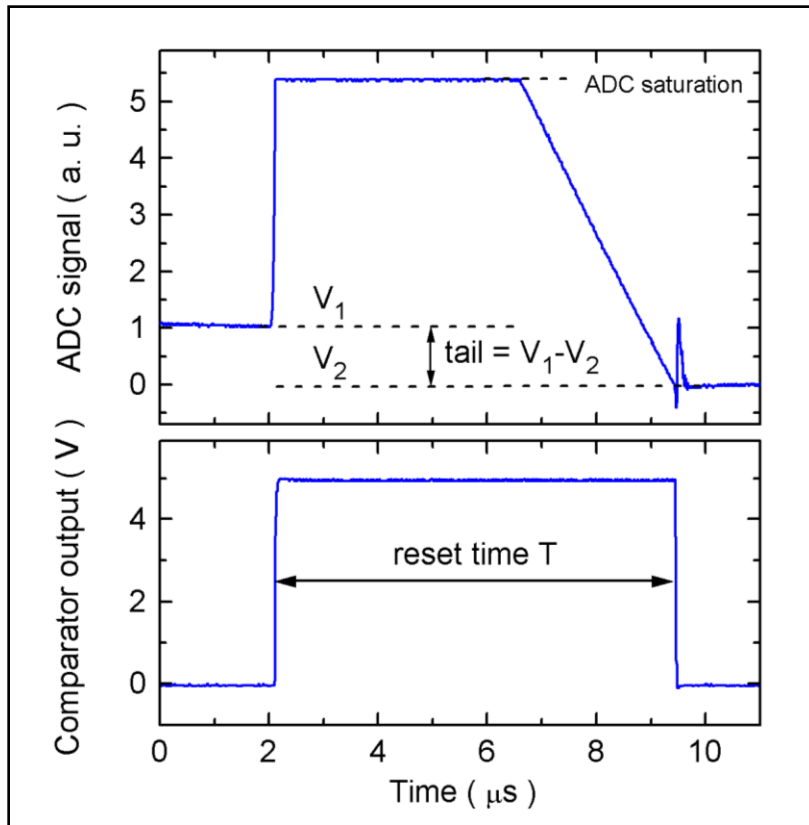


Saving the original data produces ~5 ÷ 30 TB / experiment
 Disk server (100 TB) is always almost full → data archived to the GRID

AGATA hybrid charge sensitive preamplifiers



Time-Over-Threshold (TOT) technique



second-order time-energy
relation

offset term

$$E = b_1 T + b_2 T^2 - k_1 (V_1 - V_2) + E_0$$

contribution of the tail due
to previous events

$E =$ energy of the large signal

$T =$ reset time

$V_1, V_2 =$ pre-pulse and post-pulse baselines

$b_1, b_2, k_1, E_0 =$ fitting parameters

Within ADC range



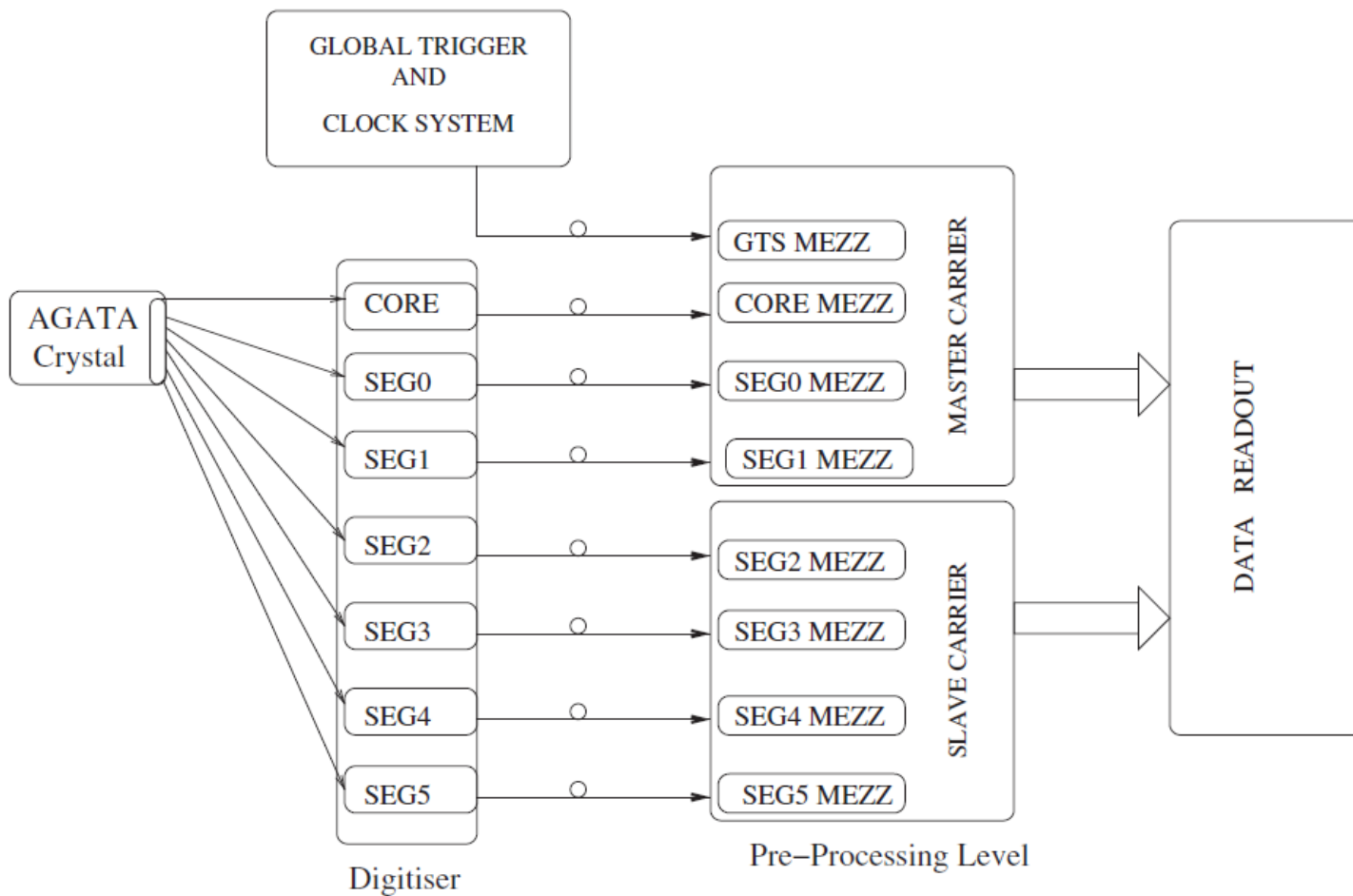
standard "pulse-height mode" spectroscopy

Beyond ADC range



new "reset mode" spectroscopy

Schematic view of AGATA front-end electronics and data readout

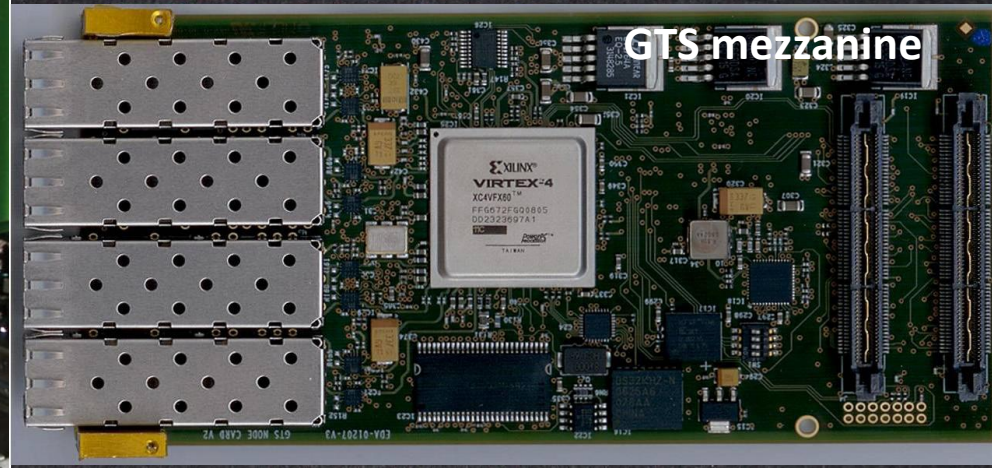
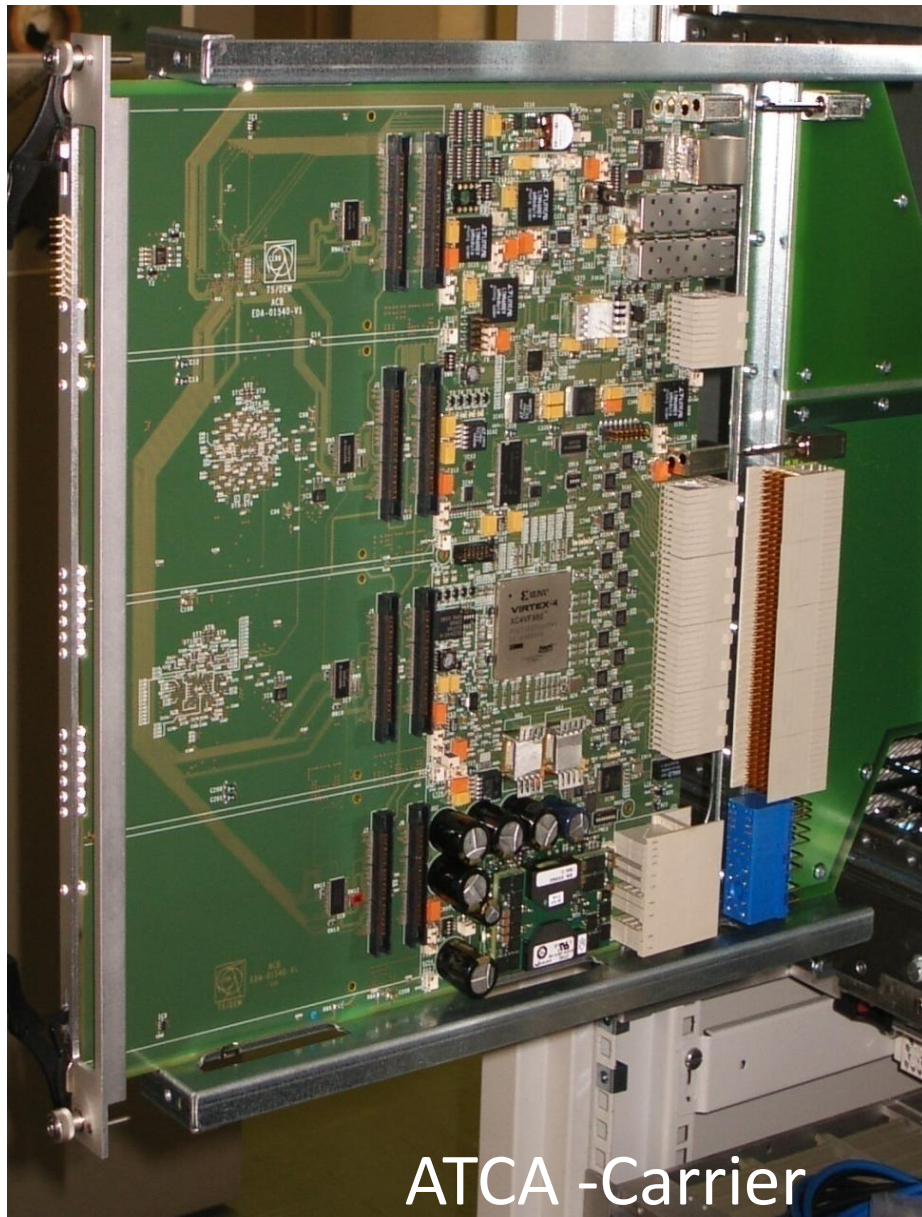


The AGATA Digitiser

- 100 MS/s
 - max frequency correctly handled is 50 MHz (Nyquist)
- 14 bits
 - Effective number of bits is ~ 12.5 (SNR ~ 75 db)
- 2 cores and 36 segments (in 6 boards)
- Core 2 ranges 5, 20 MeV nominal
- Segments either high or low gain
- The digitized samples are serialized and transmitted via optical fibre (1/channel) to the preprocessing electronics. Transmission rate is 2 Gbit/s on each of the 38 fibres.
- Power consumption 240 W
- Weight 35 kg
- Inspection lines and CFD Output



ATCA Pre-Processing Electronics



The Pre-Processing is the first level that can interact with the Global Trigger through the GTS mezzanine. It receives, and send to the Digitizer, the Global clock synchronizing the system.

GTS : the system coordinator

All detectors operated on the same 100 MHz clock

Downwards

100 MHz clock + 48 bit Timestamp (updated every 16 clock cycles)

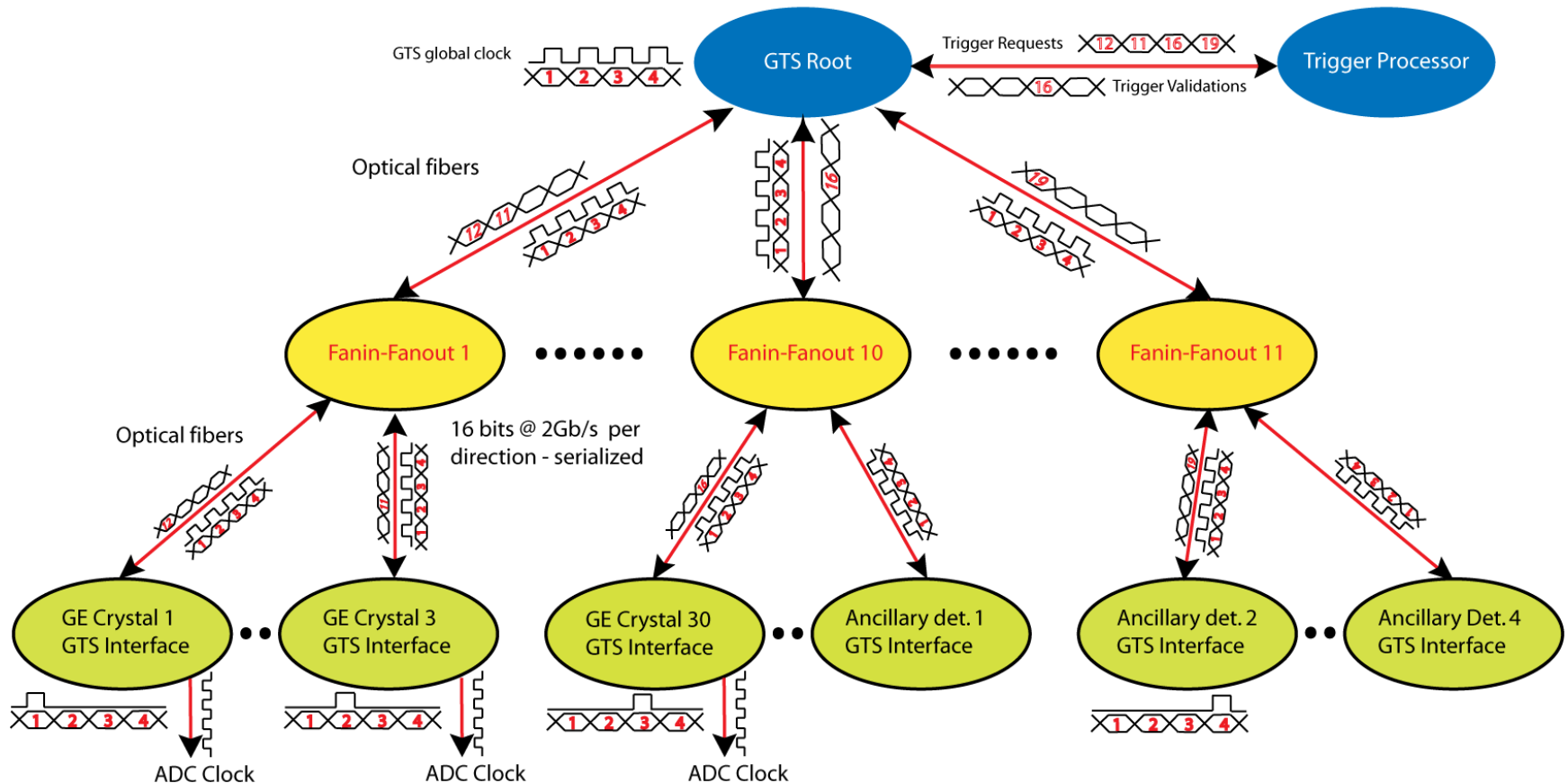
Upwards

trigger requests, consisting of address (8 bit) and timestamp (16 bit)

max request rate 10 MHz total, 1 MHz/detector

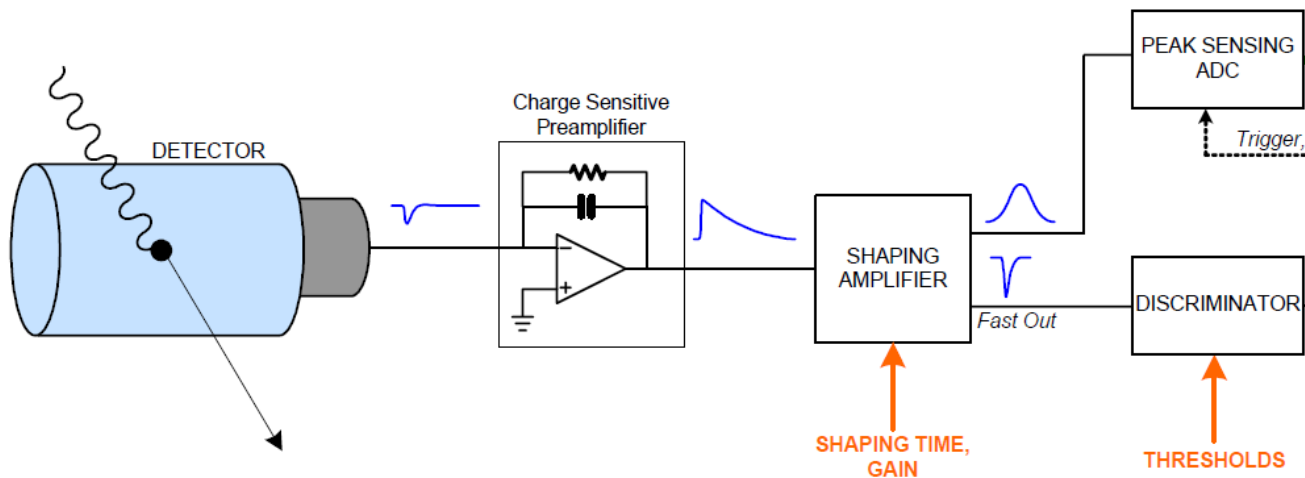
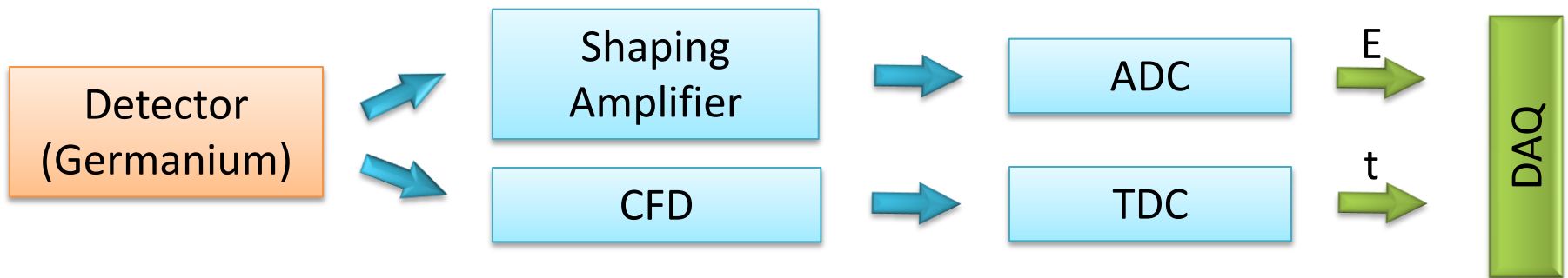
Downwards

validations/rejections, consisting of request + event number (24 bit)



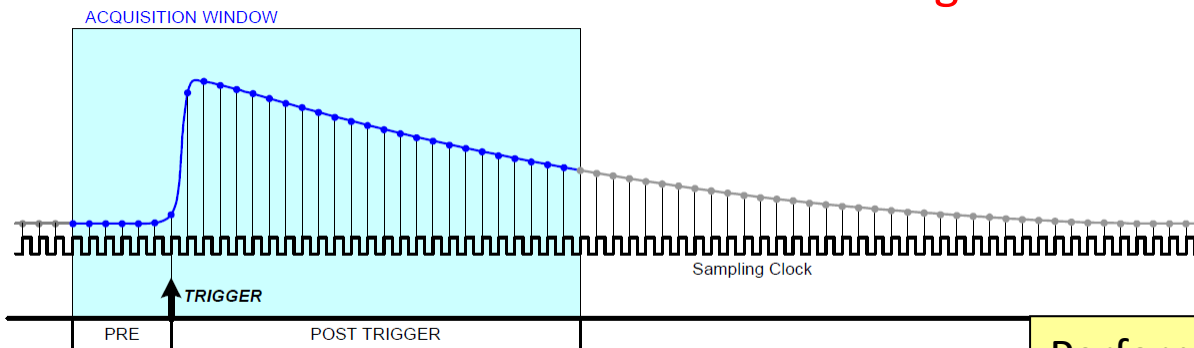
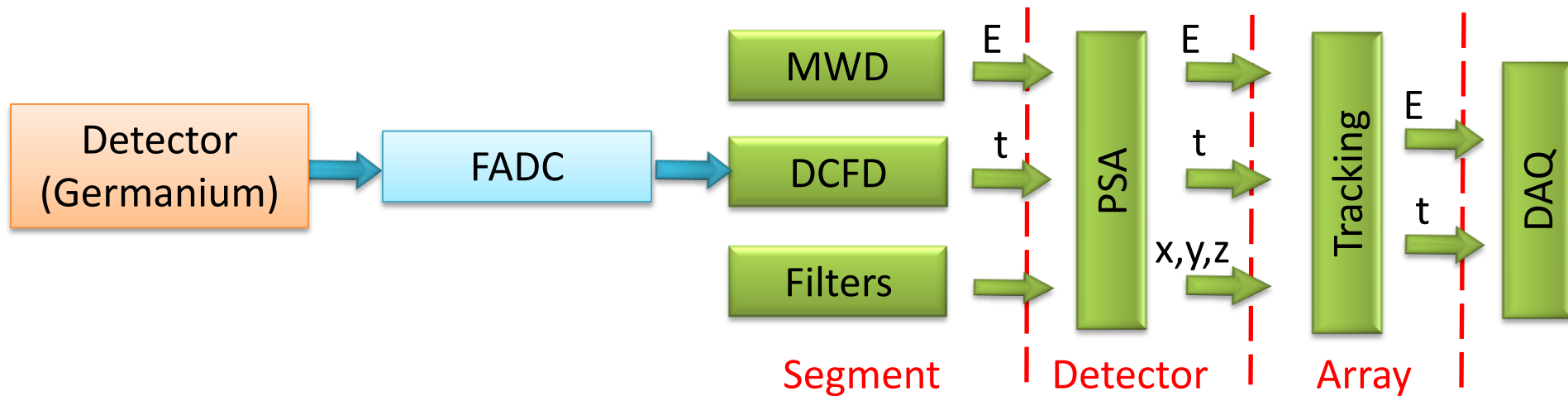
Analogue vs Digital Electronics

Standard Arrays



Analogue vs Digital Electronics

AGATA



Performance comparable to best analog electronics.
Higher count rate capabilities

Digital processing of signals

The energy is obtained via trapezoidal filter (or *Moving Window Deconvolution, MWD*)

A.Georgiev and W. Gast, IEEE Trans. Nucl. Sci., 40(1993)770

V.T.Jordanov and G.F.Knoll, Nucl.Instr.Meth., A353(1994)261

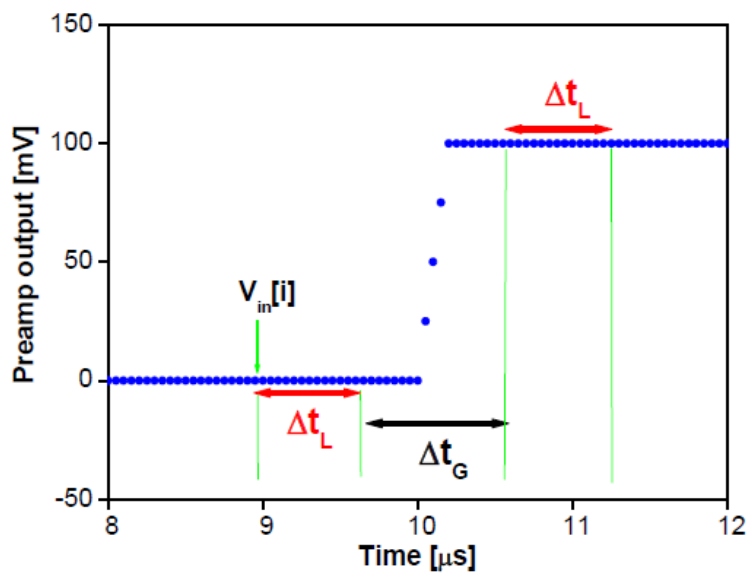


Fig. 6.26. Trapezoidal filter parameters.

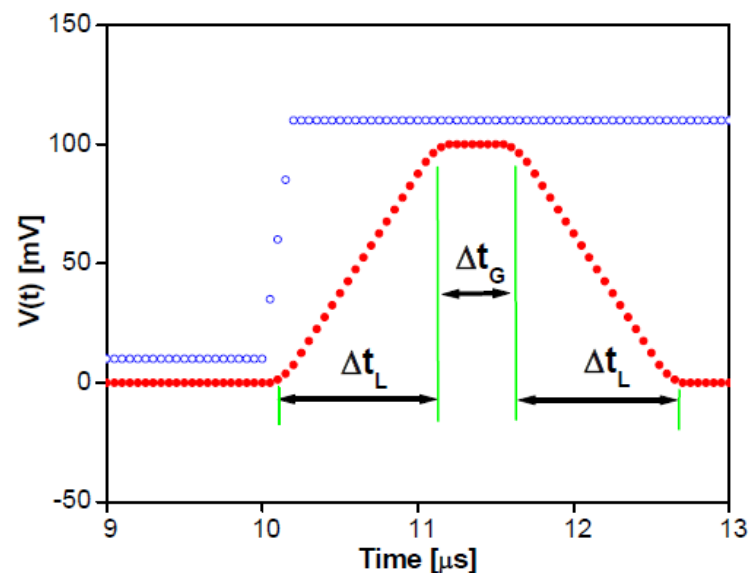


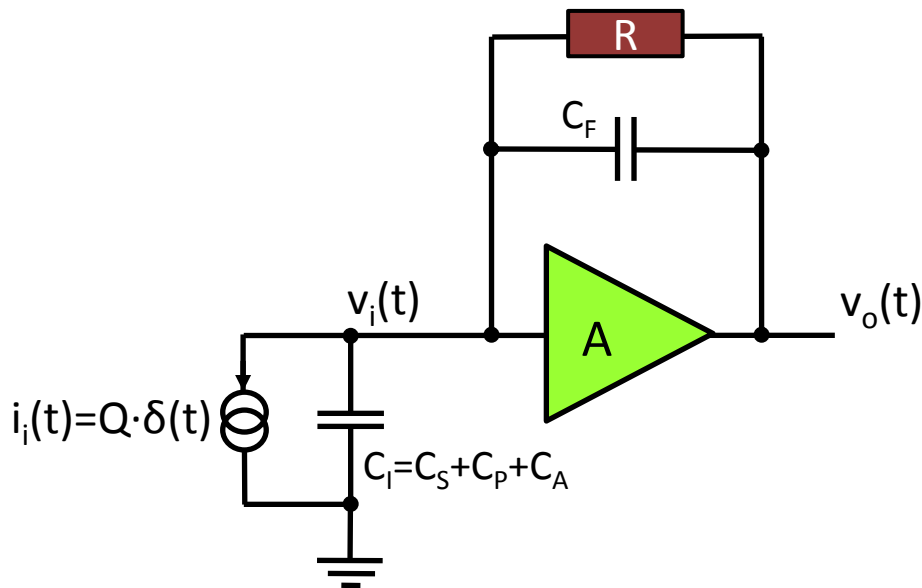
Fig. 6.27. Trapezoidal filter output.

- 1)
$$V_{av1}[i] = \frac{1}{L} \sum_{j=0}^{L-1} V_{in}[i+j]$$
- 2)
$$V_{av2}[i] = \frac{1}{L} \sum_{j=0}^{L-1} V_{in}[L+G+i+j]$$
- 3)
$$V_{out}[i] = V_{av2}[i] - V_{av1}[i]$$

Signal amplitude =
value at the top –
value of the baseline

“Deconvolution” of Ge signals

- Signals from Ge preamplifiers are, ideally, exponentials with only one decay constant

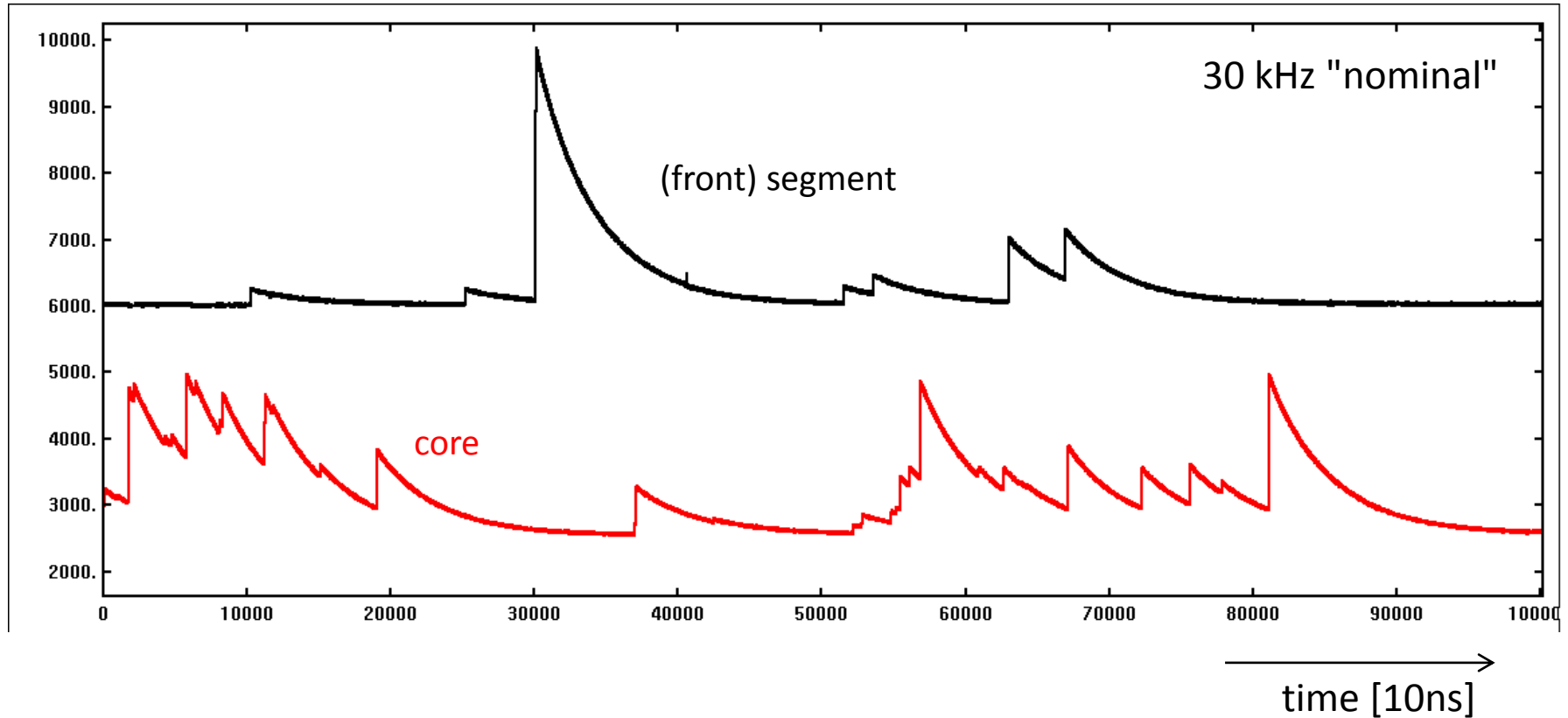


In practice the output exponential is produced in stages :

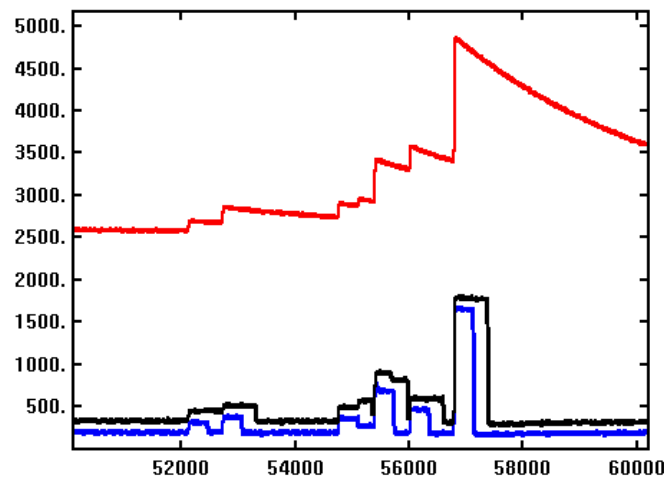
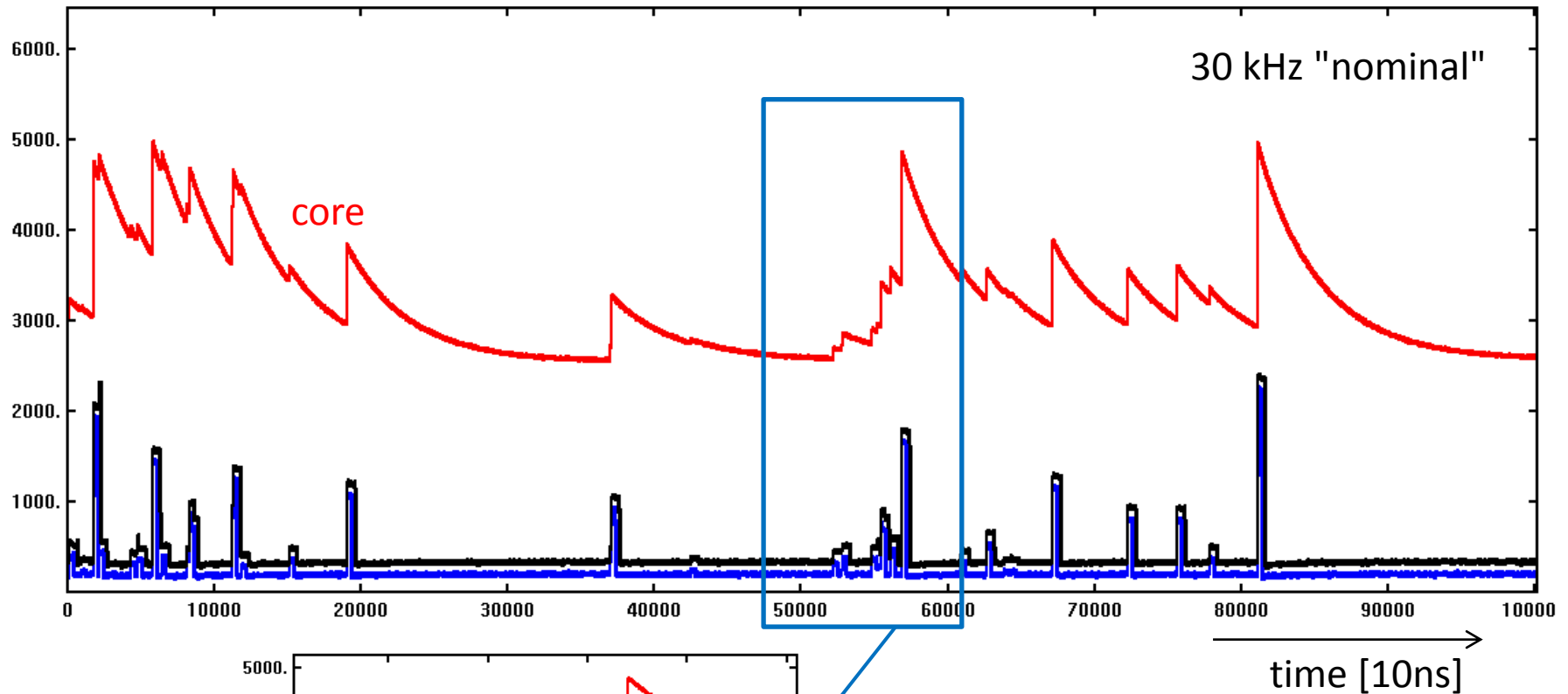
- RC_F charge loop with decay constant $\tau_0 \sim 1$ ms
- CR differentiation to reduce the decay constant to $\tau_1 \sim 50$ μ s
- P/Z cancellation to remove the undershoot and the long recovery (with $\tau = \tau_0$) due to the differentiation of the first exponential.

- Task of the **deconvolution** is to remove the exponential to recover the original $\delta(t)$ at the input of the preamplifier
- **Trapezoidal shaping** is then just an integration followed by delayed subtraction followed by a moving average
- In practice **Trapezoidal shaping** is the optimum shaping if the noise is white and the collection time (width of the “delta”) varies a lot as in the large volume semi-coax Ge AGATA detectors

Signal processing at high counting rates



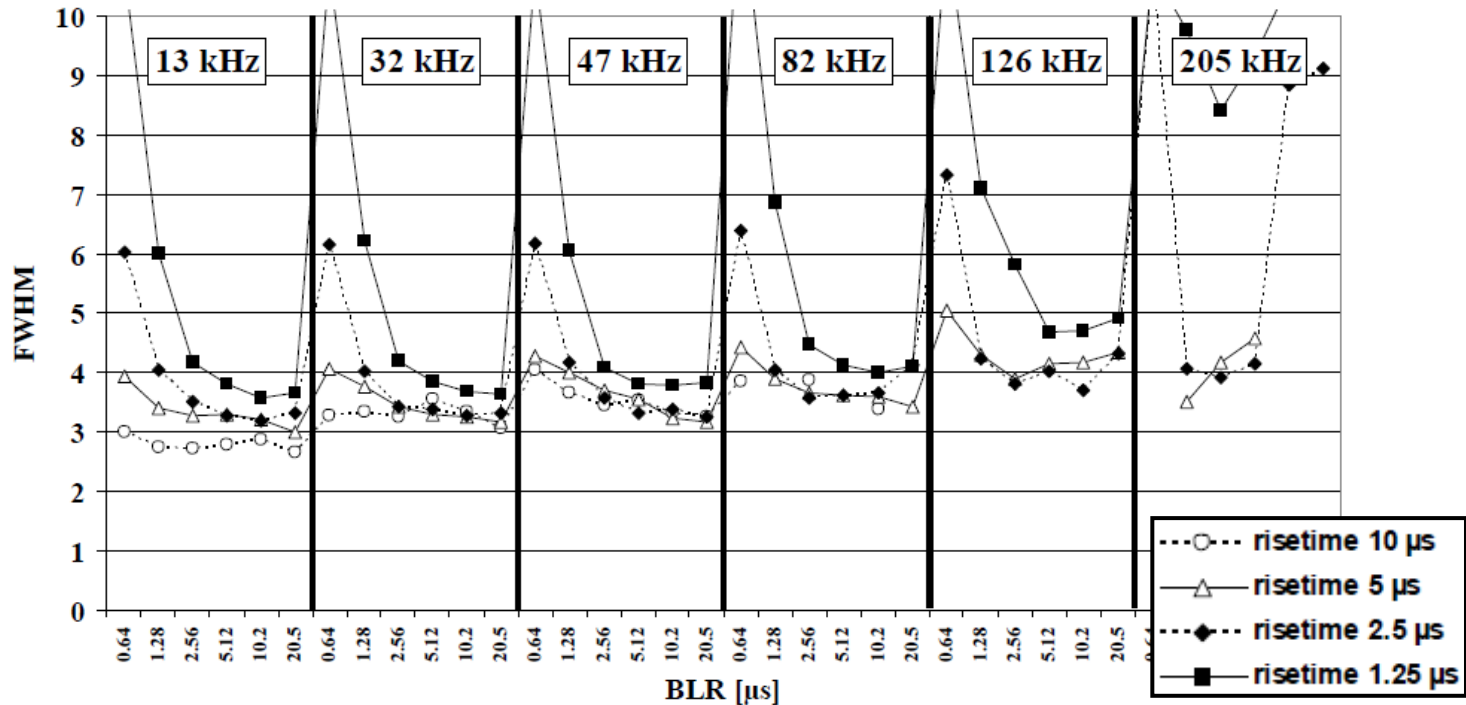
Signal processing at high counting rates



MWD amplitude:
risetime 5 μ s
risetime 2.5 μ s

Singles rates and shaping time

6 different rates x 4 trapezoid risetimes x 6 BLR lengths



Singles rates and shaping time

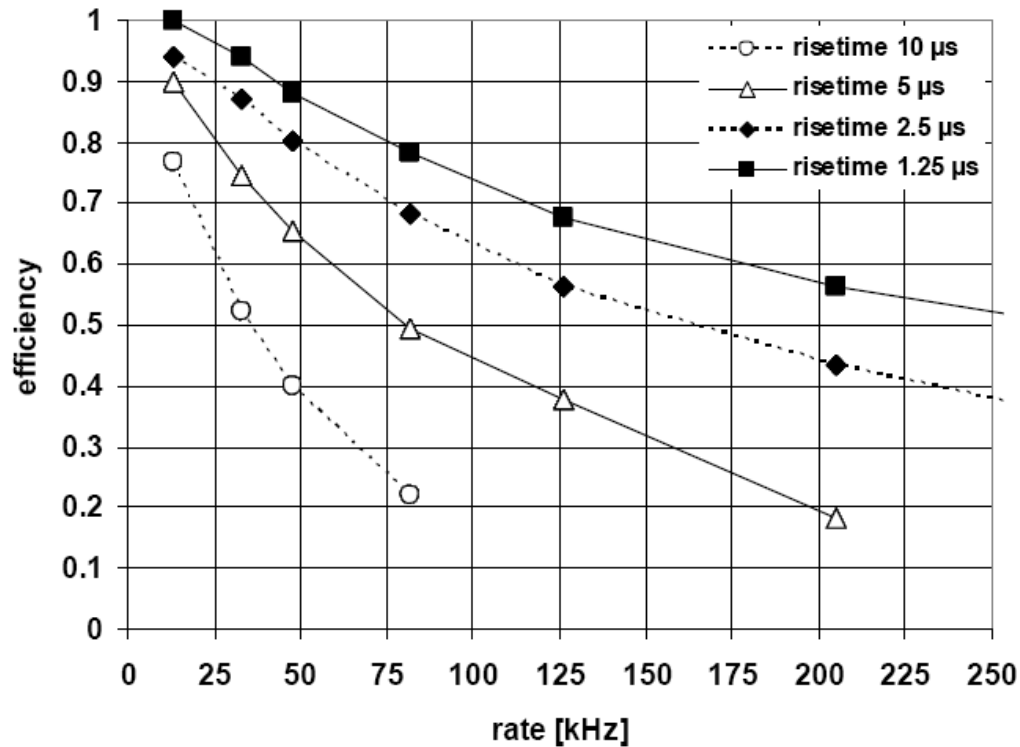


Fig. 1. Efficiency as a function of rate.



AGATA Data Processing

(from raw data to reconstructed "good" gamma rays)

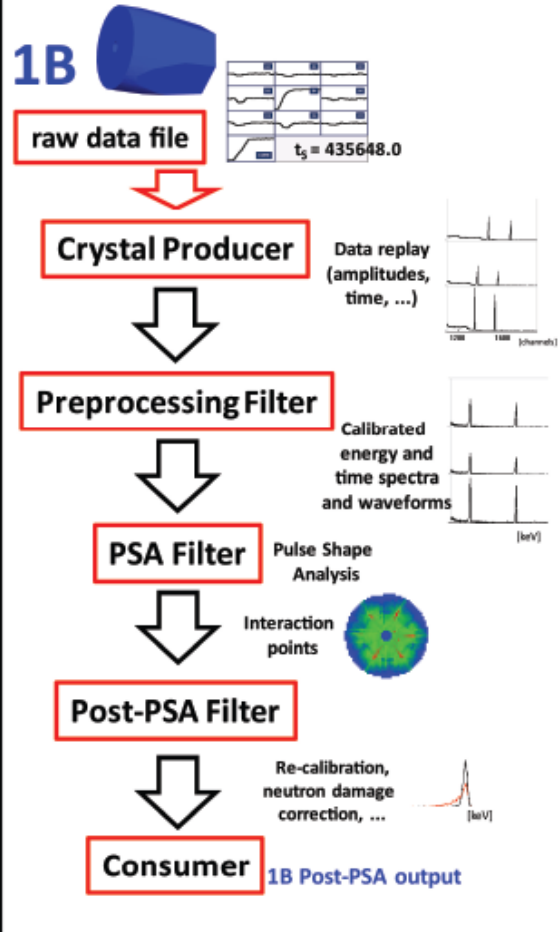
Offline data processing = Online data processing

Structure of Data Processing

Local Level Processing

1R 
...

1G 
...



...

1R Post-PSA output

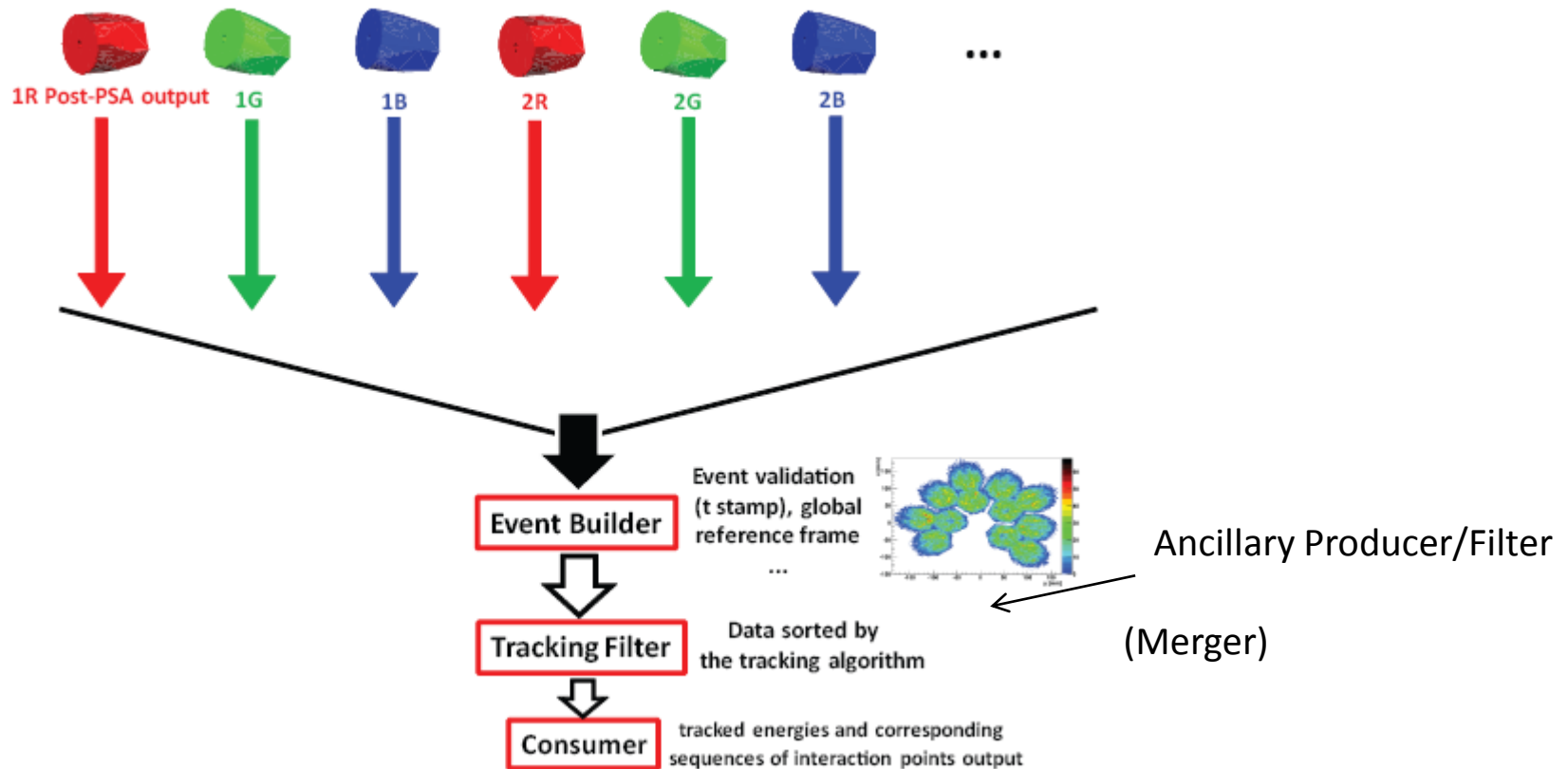
1G Post-PSA output

1B Post-PSA output

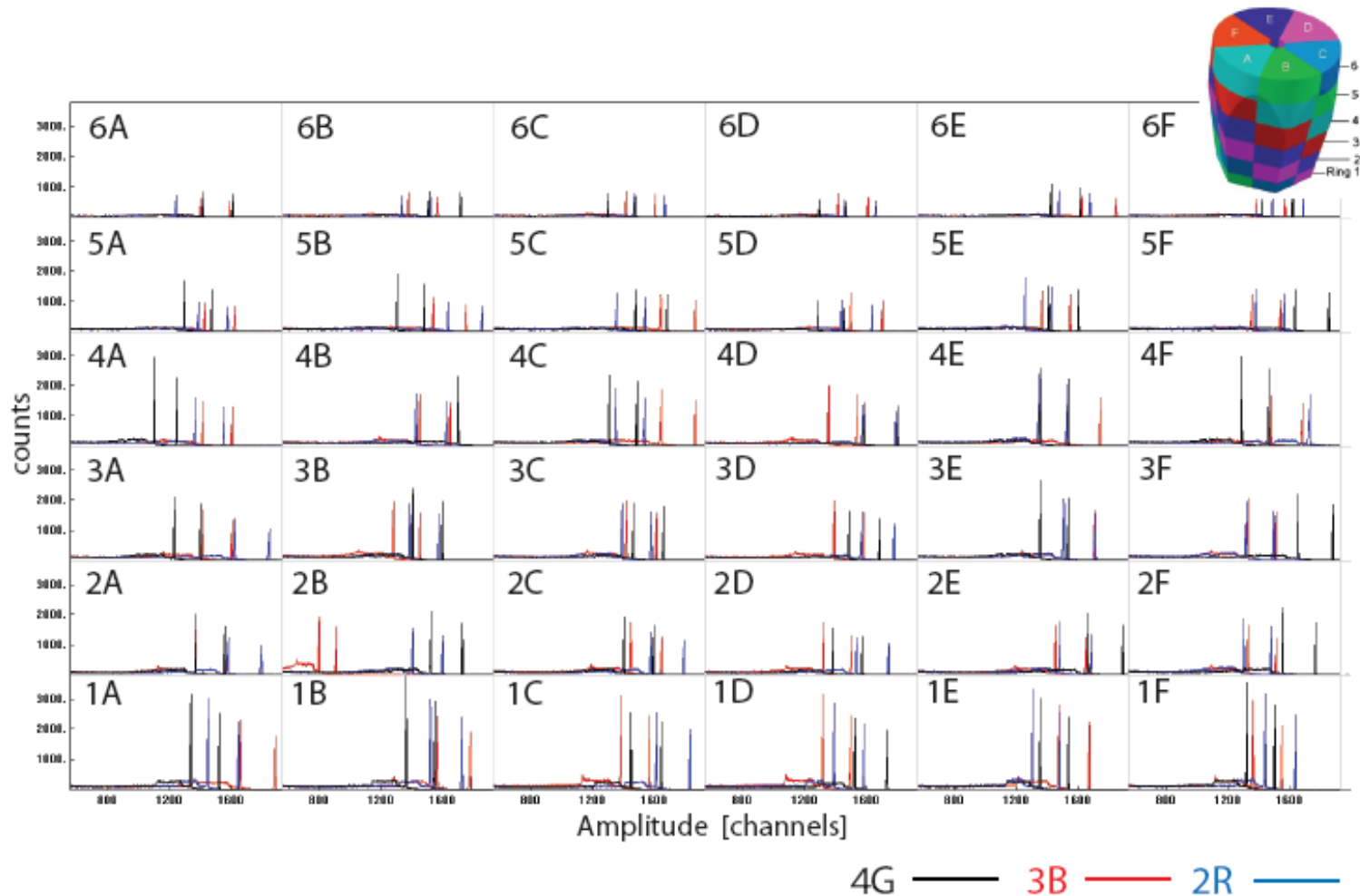
```
Chain 4 1B/
Producer CrystalProducerATCA
Filter PreprocessingFilterPSA
Filter PSAFilterGridSearch
Consumer BasicAFC
```

Structure of Data Processing

Global Level Processing



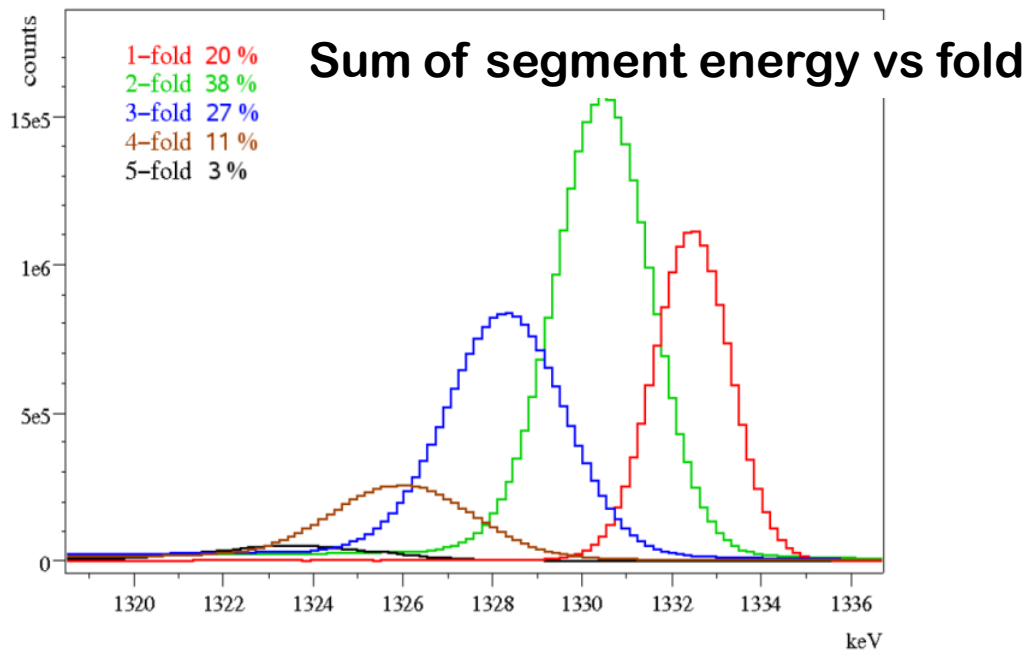
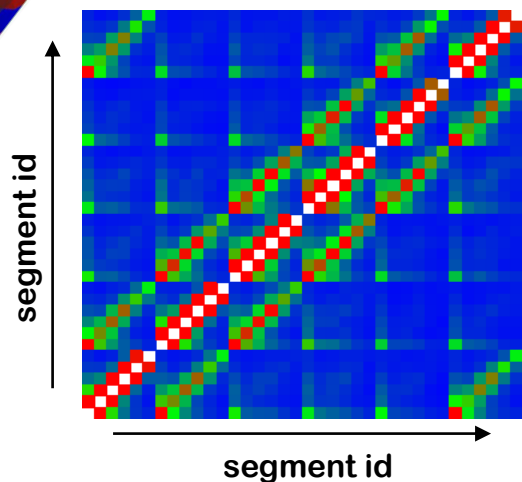
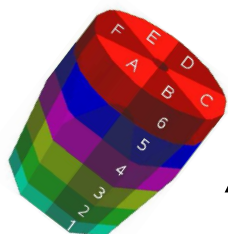
Data preparation to the PSA: energy calibrations



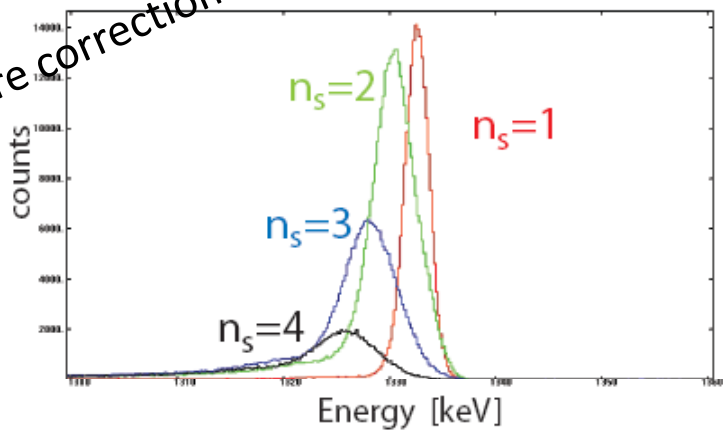
Calibration of traces: from calibrations of amplitudes and MWD parameters

Data preparation to the PSA: Cross-talk Correction

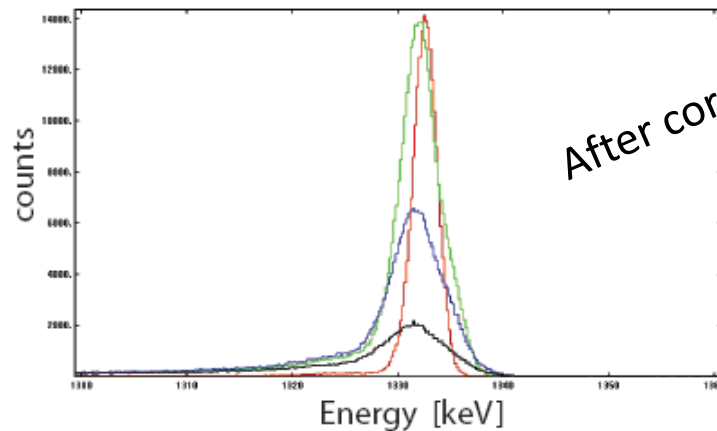
Generate strong energy shifts proportional to the segment fold



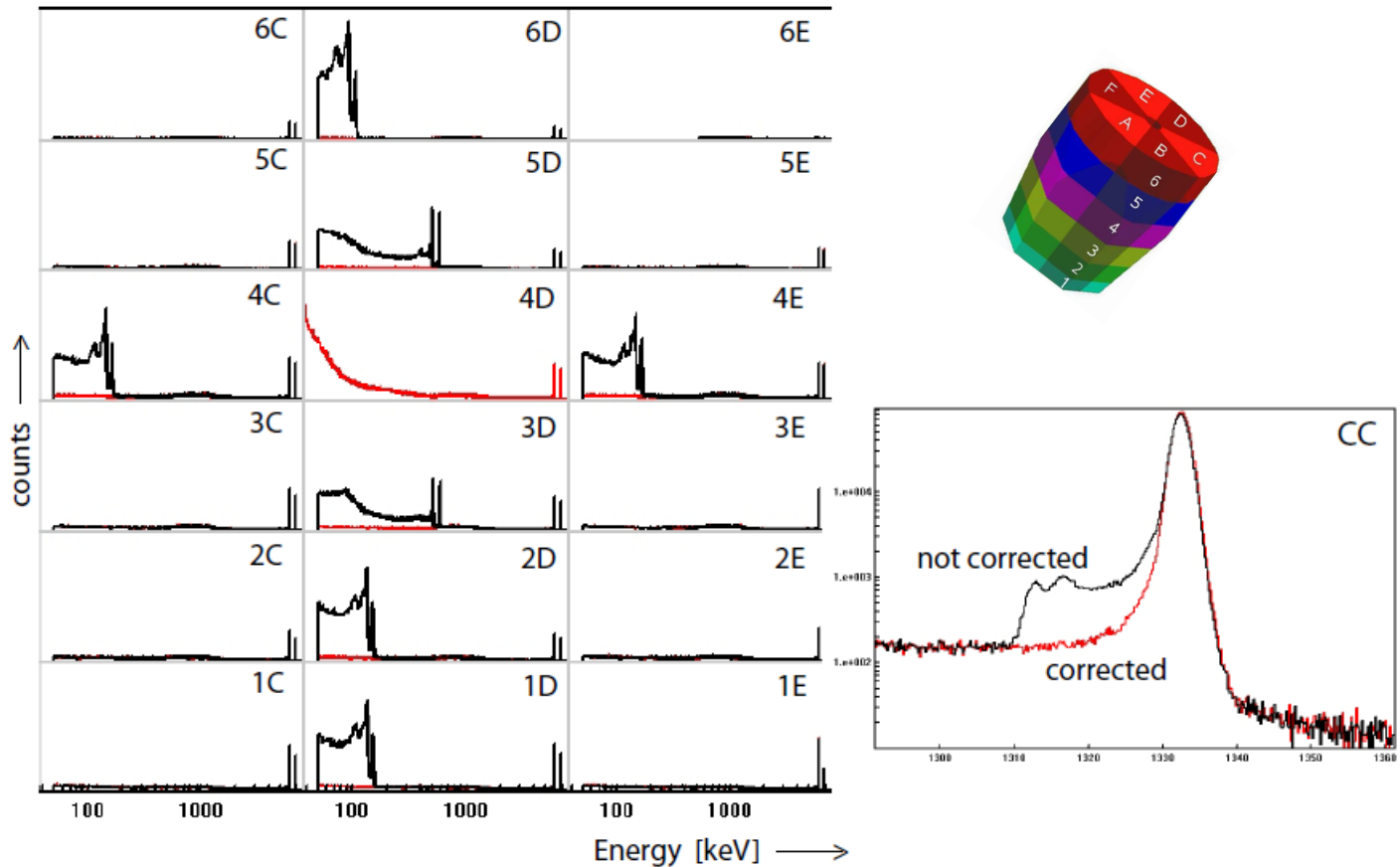
Before correction



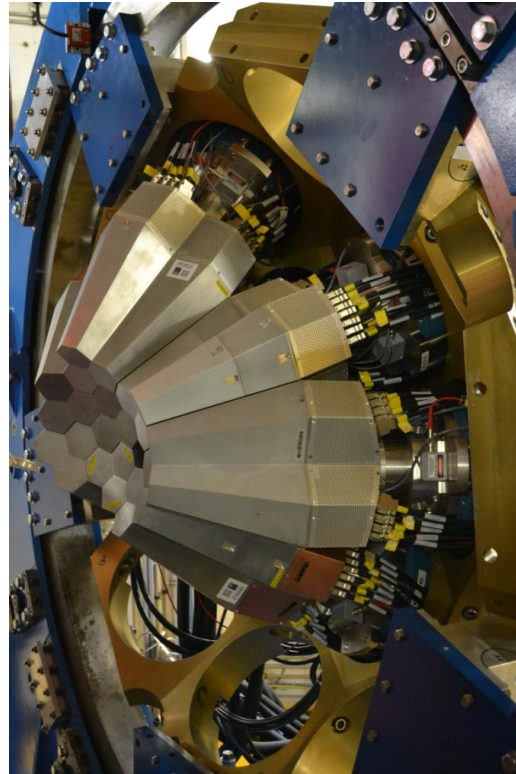
After correction



Data preparation to the PSA: recovery of missing segment

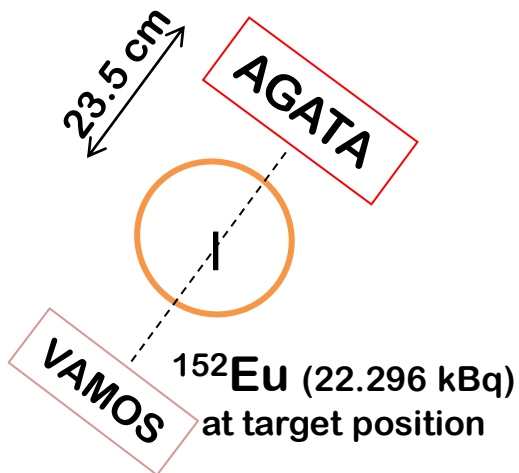


Some results from the commissioning runs in GANIL

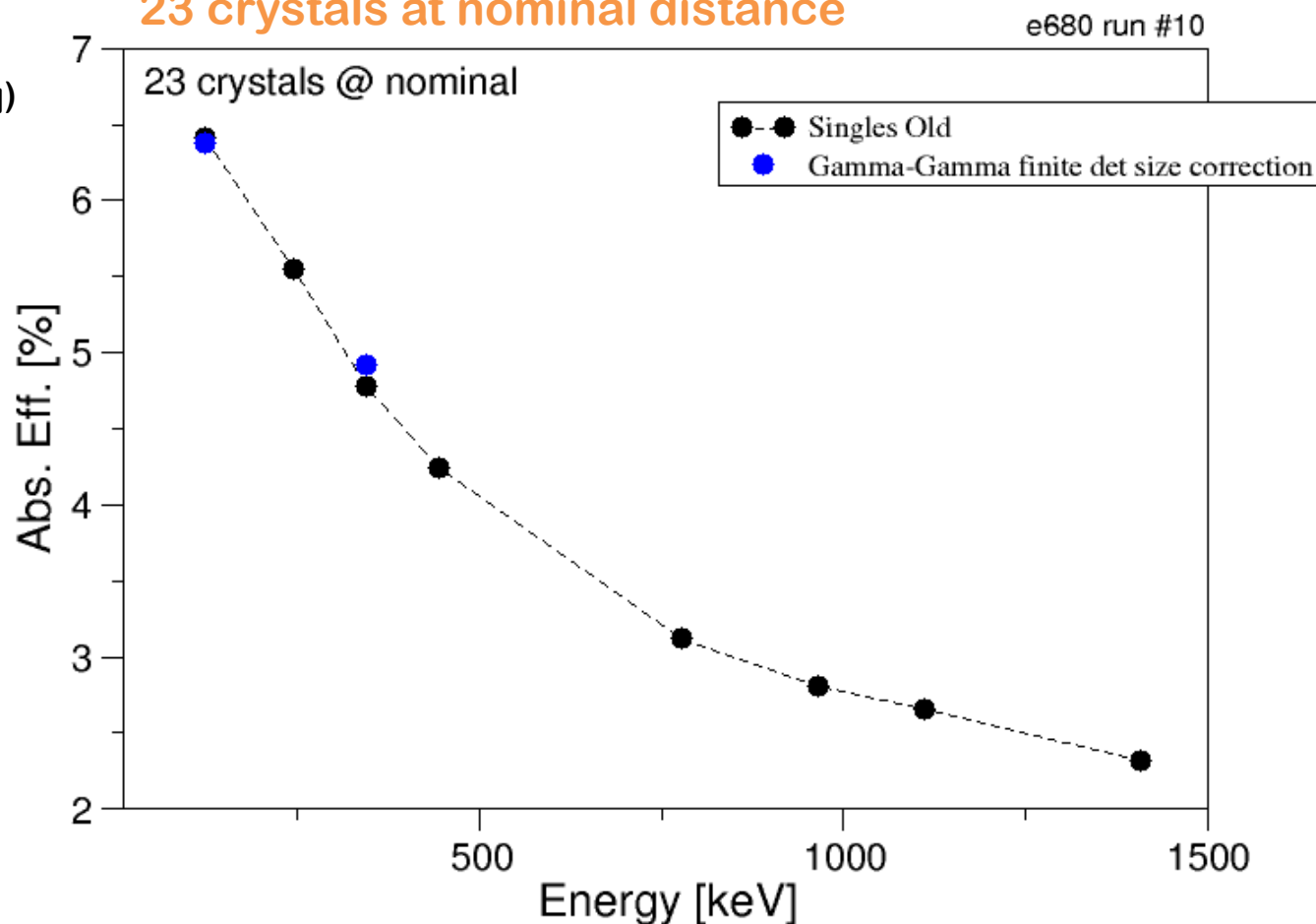


Absolute efficiency vs Energy

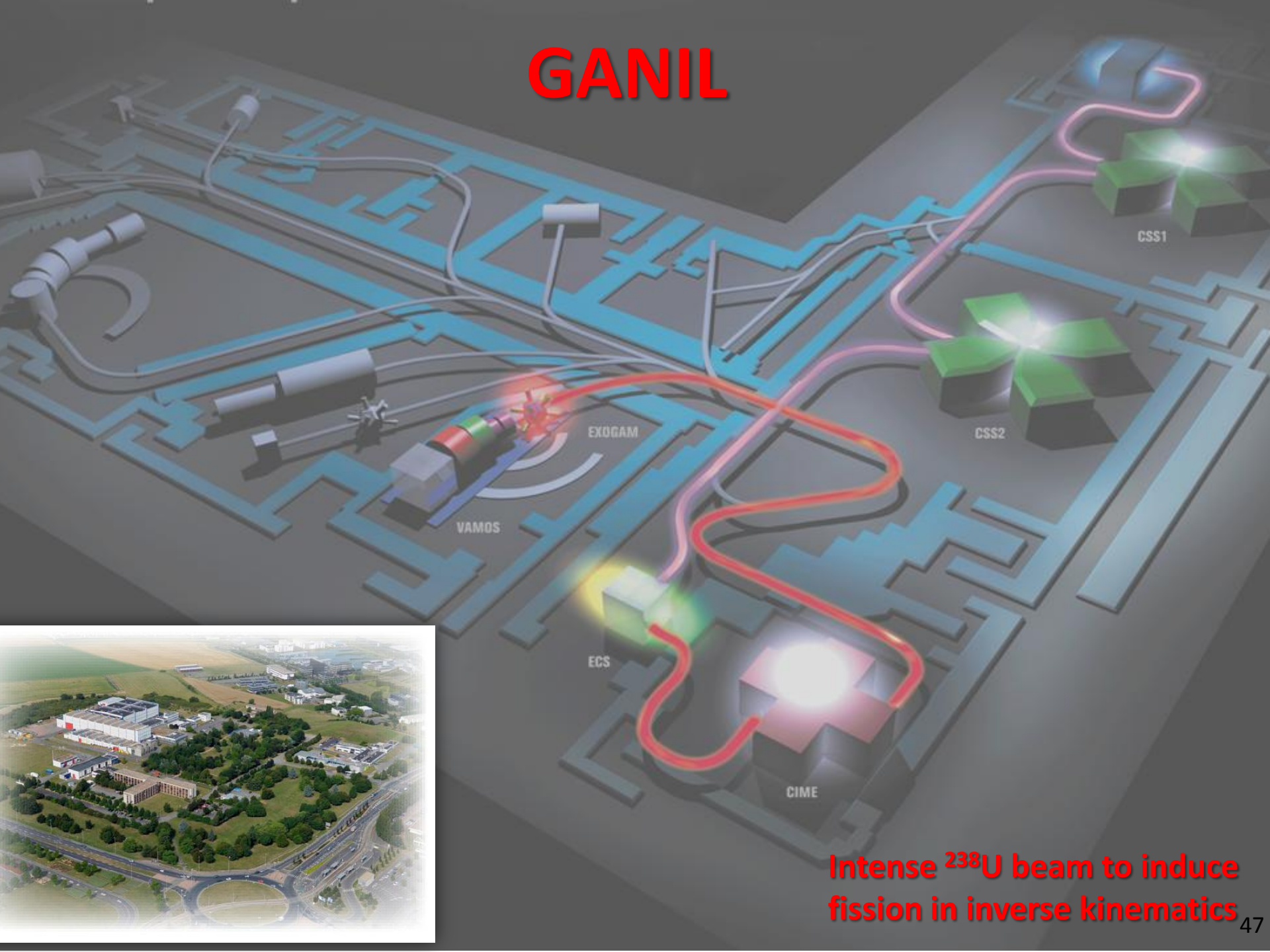
AGATA Cores triggering through VAMOS electronics
(same trigger partitions as in-beam experiments)



Core Common Abs. Efficiency
23 crystals at nominal distance

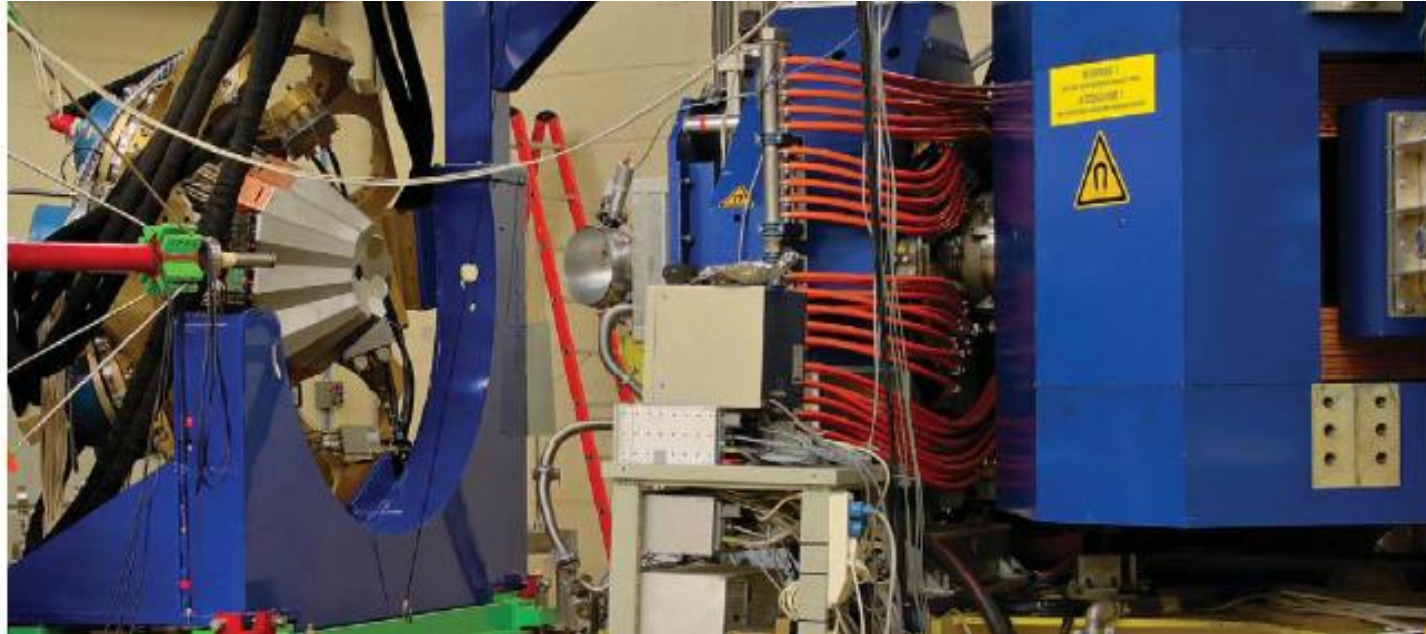


GANIL

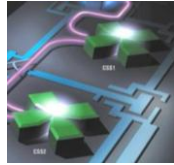


Intense ^{238}U beam to induce fission in inverse kinematics

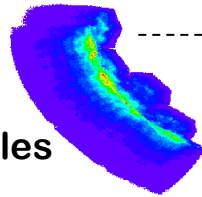
Experimental setup: ~~AGATA + VAMOS @ GANIL~~ PRISMA ~~LNL~~



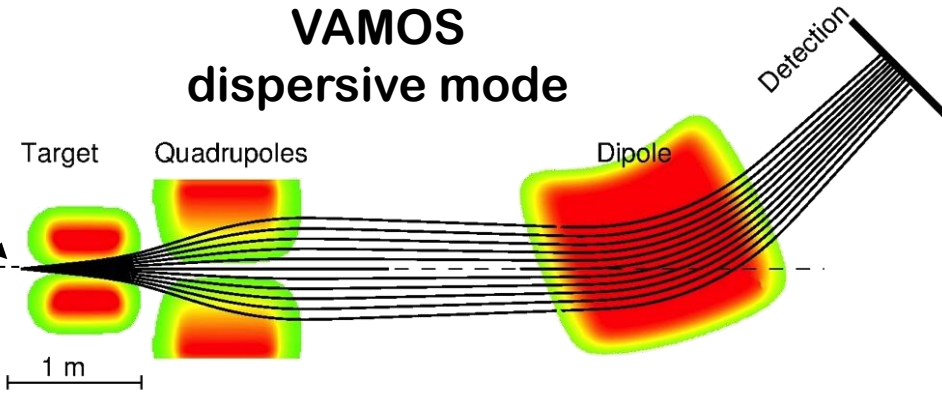
AGATA + VAMOS @ GANIL



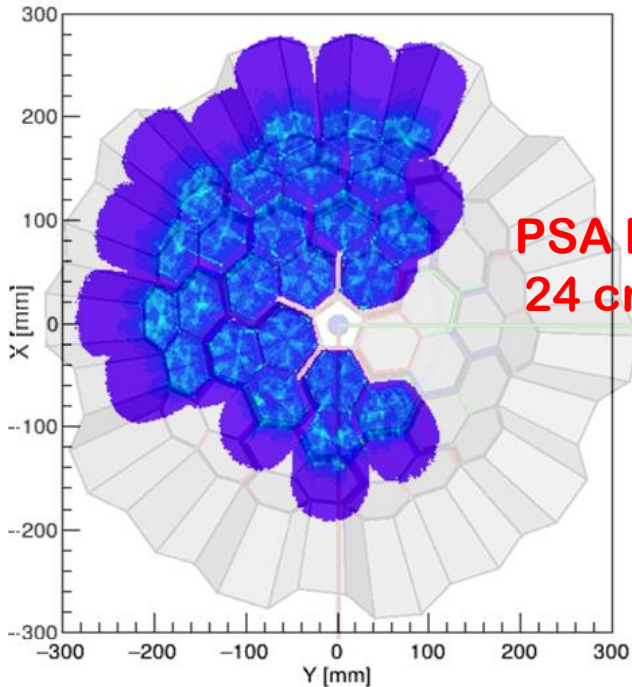
AGATA
at backward angles



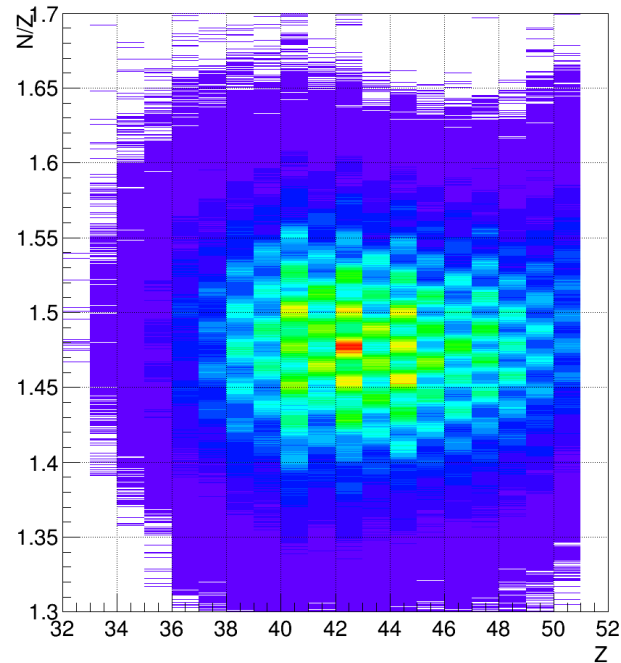
beam



Event by event: AGATA: γ energy and interaction points; VAMOS: A, Z, β



PSA hits for
24 crystals



**$^{238}\text{U}+^9\text{Be}$ @ 6.6 MeV/u
commissioning run
December 2014**

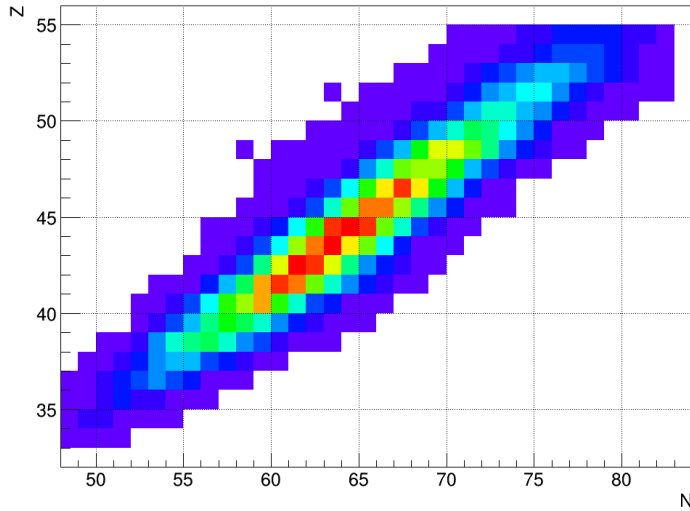
γ rays from isotopically id. fission fragments

$^{238}\text{U}+^9\text{Be}$ @ 6.6 MeV/u

the fission nuclide chart

AGATA+VAMOS commissioning run, December 2014

$^{238}\text{U}+^9\text{Be}$ (6.6 MeV)



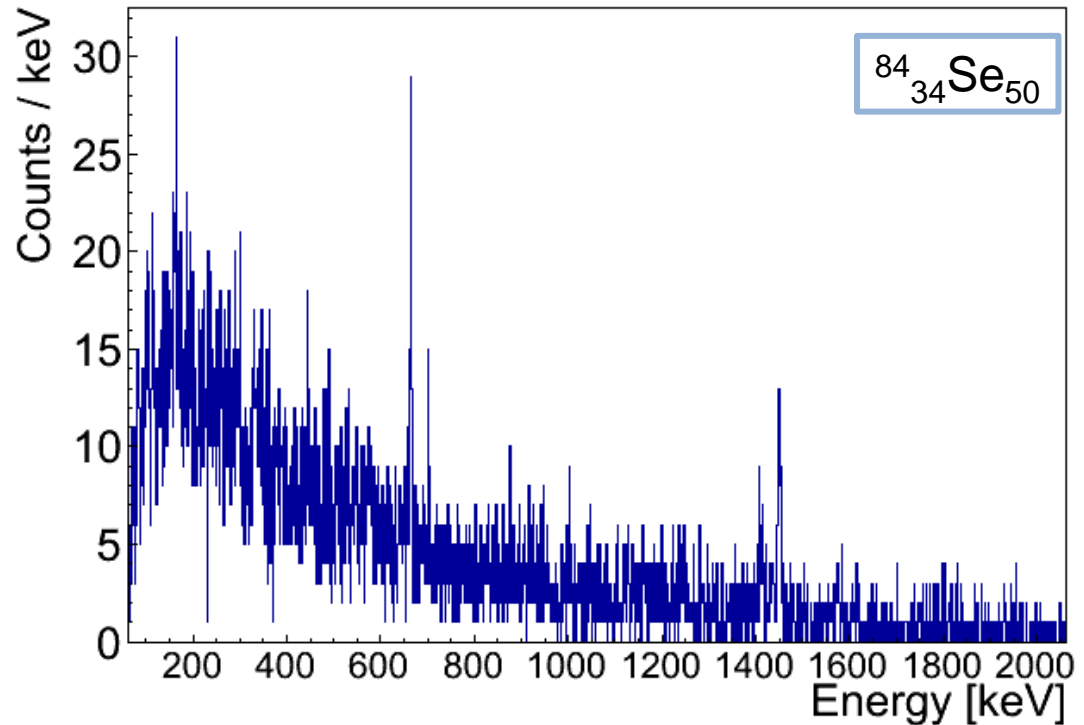
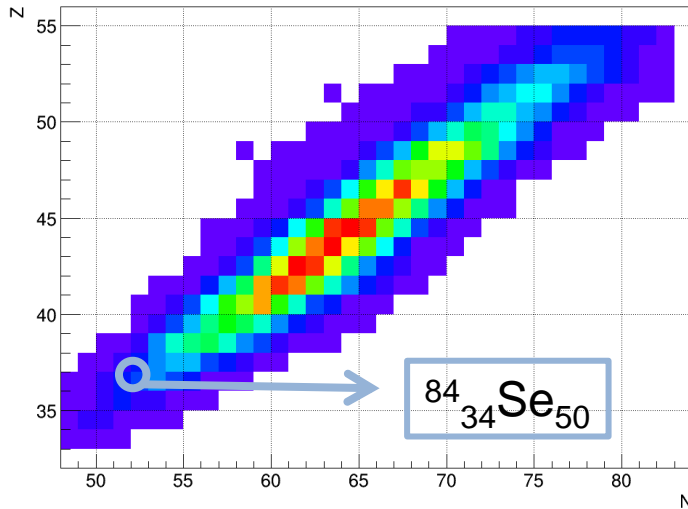
γ rays from isotopically id. fission fragments

$^{238}\text{U}+^9\text{Be}$ @ 6.6 MeV/u

the fission nuclide chart

AGATA+VAMOS commissioning run, December 2014

$^{238}\text{U}+^9\text{Be}$ (6.6 MeV)



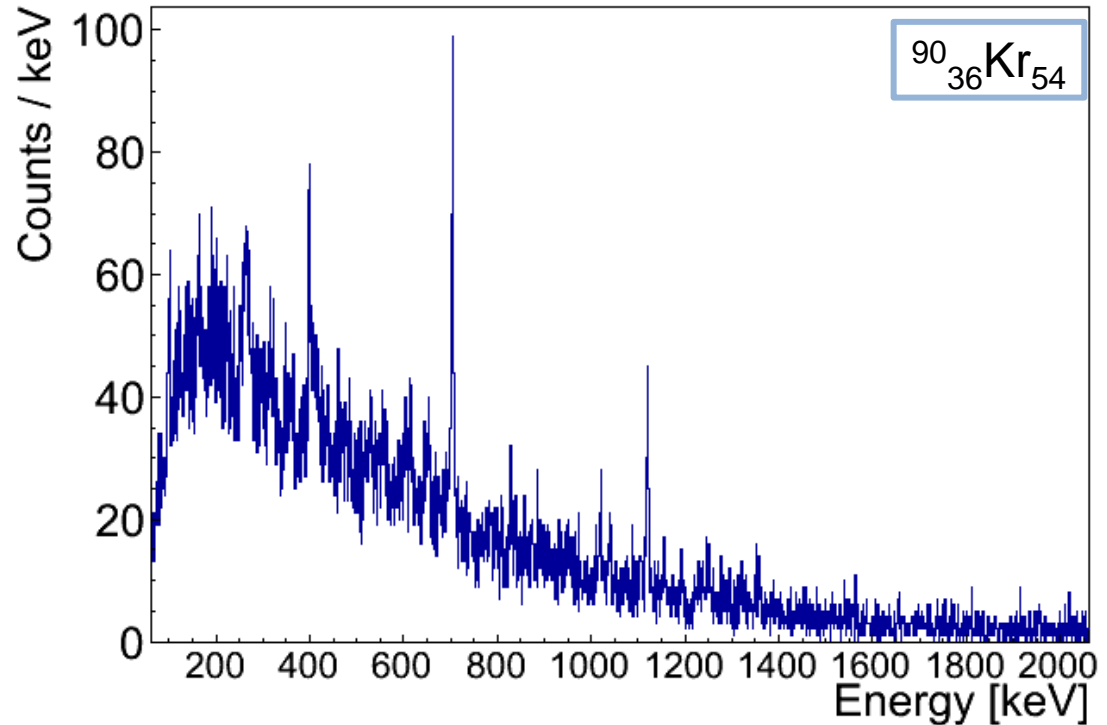
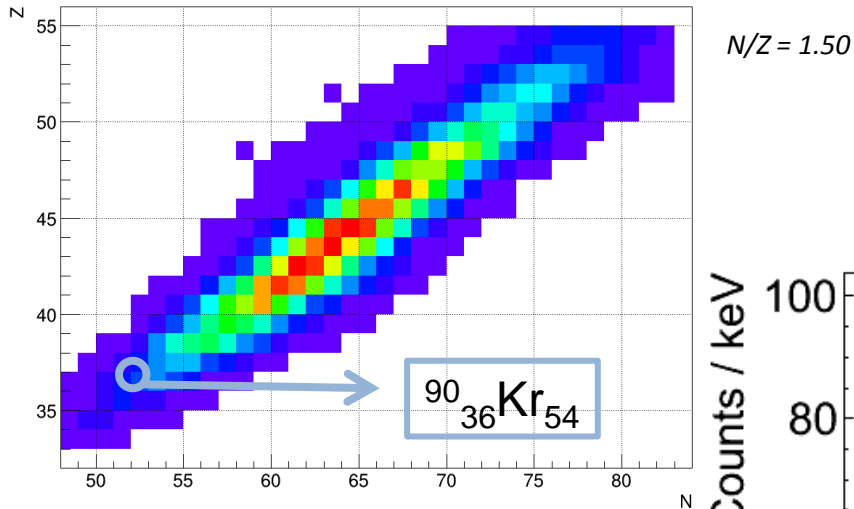
γ rays from isotopically id. fission fragments

$^{238}\text{U}+^9\text{Be}$ @ 6.6 MeV/u

the fission nuclide chart

AGATA+VAMOS commissioning run, December 2014

$^{238}\text{U}+^9\text{Be}$ (6.6 MeV)



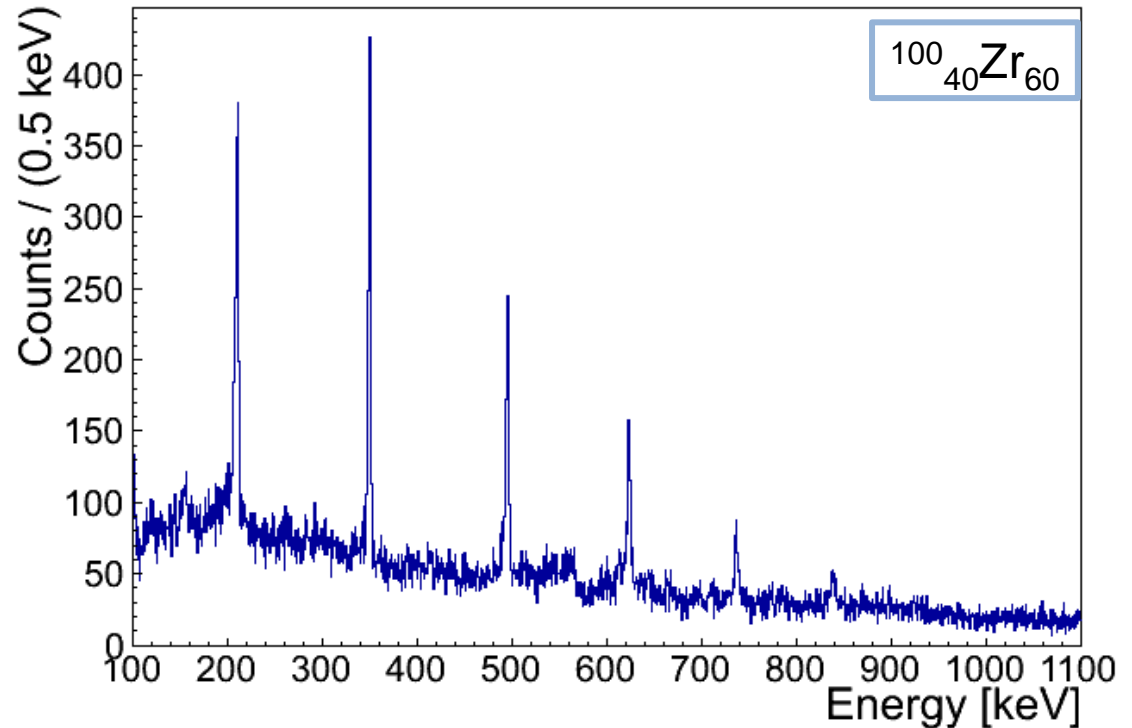
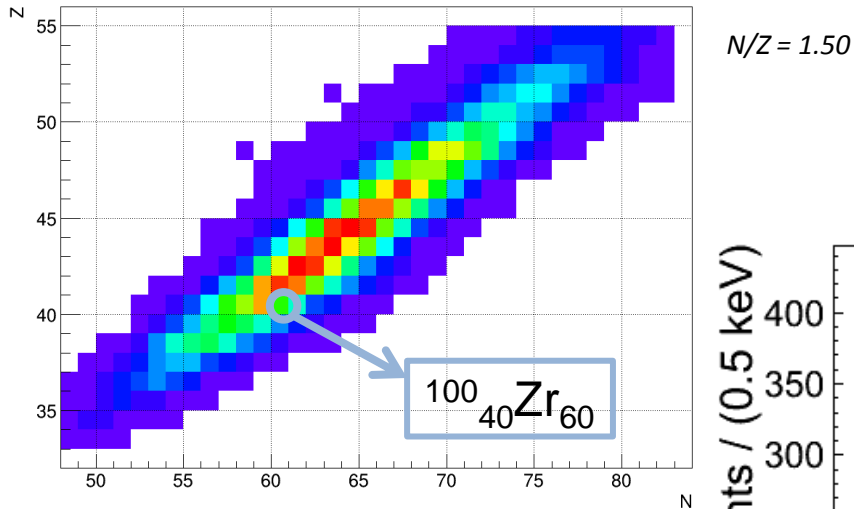
γ rays from isotopically id. fission fragments

$^{238}\text{U}+^9\text{Be}$ @ 6.6 MeV/u

the fission nuclide chart

AGATA+VAMOS commissioning run, December 2014

$^{238}\text{U}+^9\text{Be}$ (6.6 MeV)



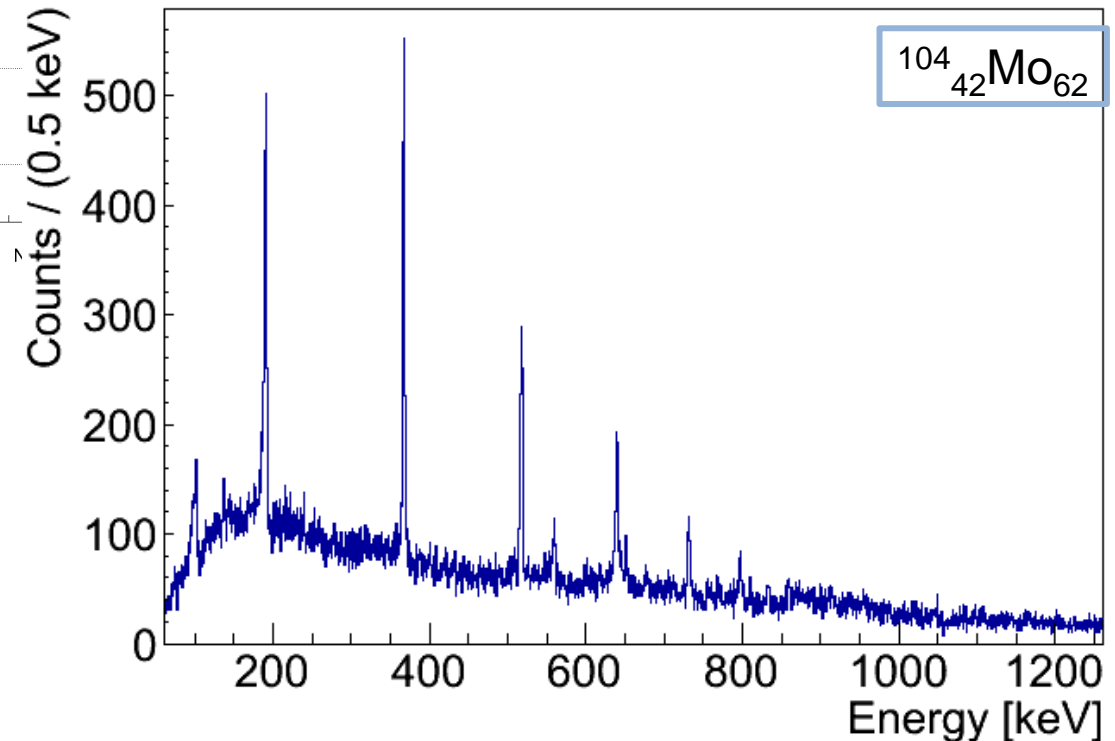
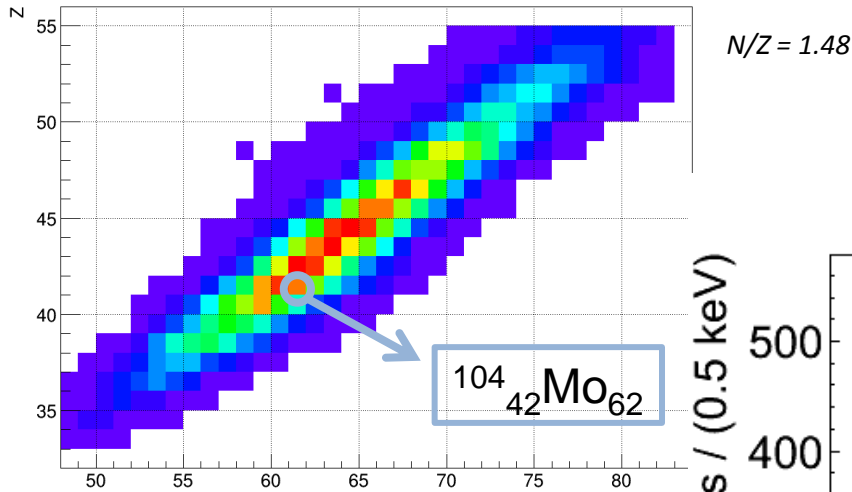
γ rays from isotopically id. fission fragments

$^{238}\text{U}+^9\text{Be}$ @ 6.6 MeV/u

the fission nuclide chart

AGATA+VAMOS commissioning run, December 2014

$^{238}\text{U}+^9\text{Be}$ (6.6 MeV)



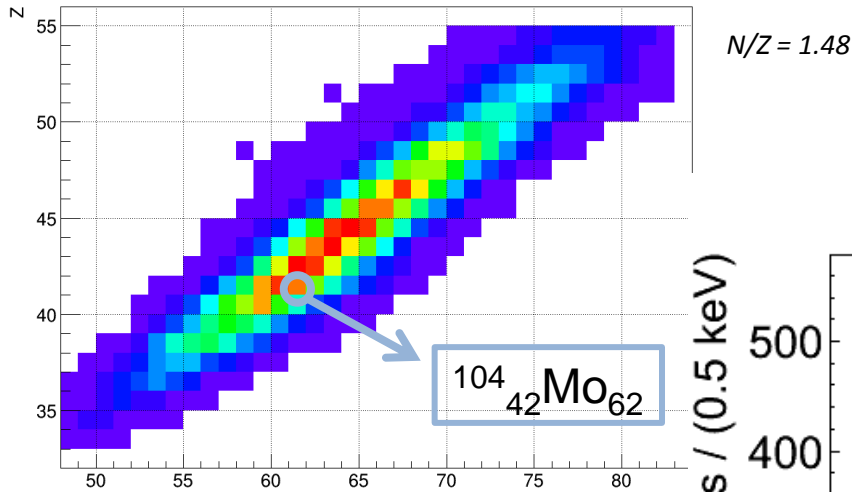
γ rays from isotopically id. fission fragments

$^{238}\text{U}+^9\text{Be}$ @ 6.6 MeV/u

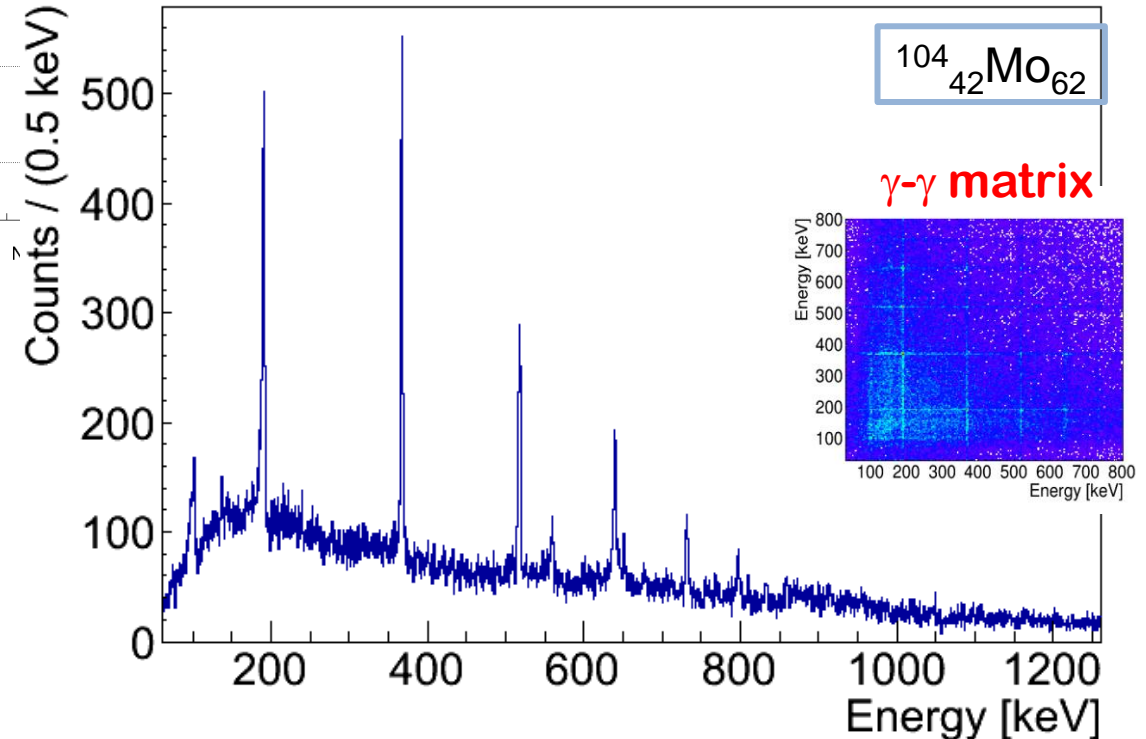
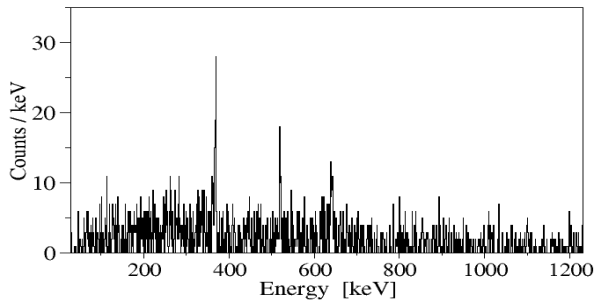
the fission nuclide chart

AGATA+VAMOS commissioning run, December 2014

$^{238}\text{U}+^9\text{Be}$ (6.6 MeV)



gate on $2^+ \rightarrow 0^+$



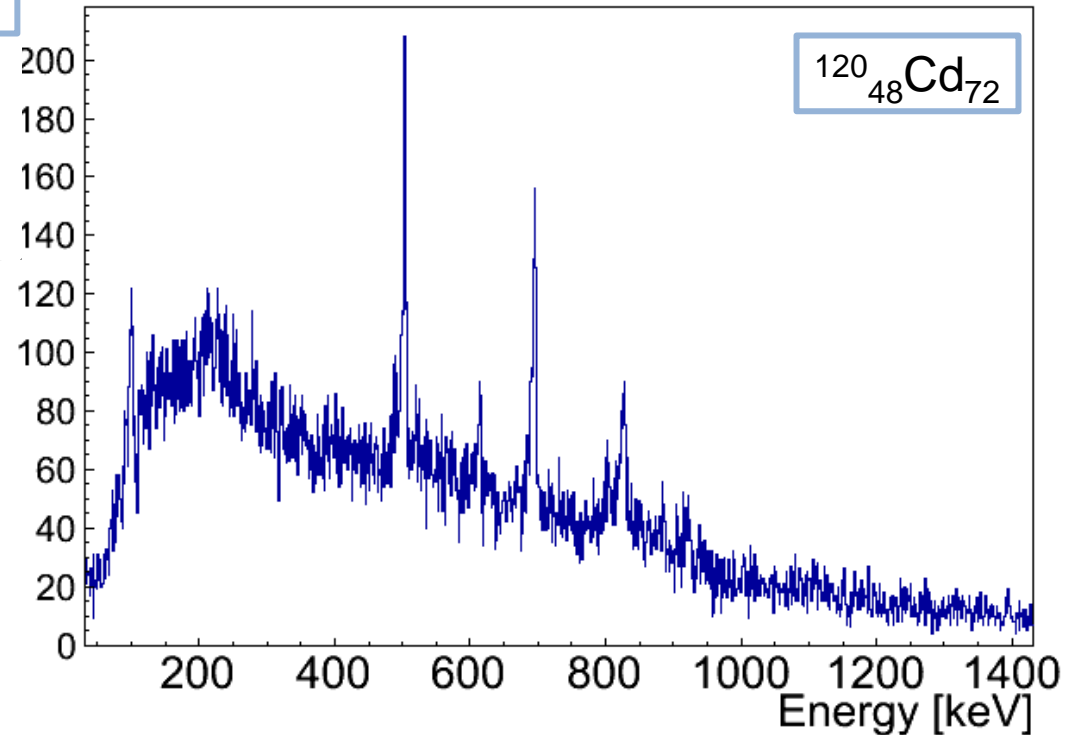
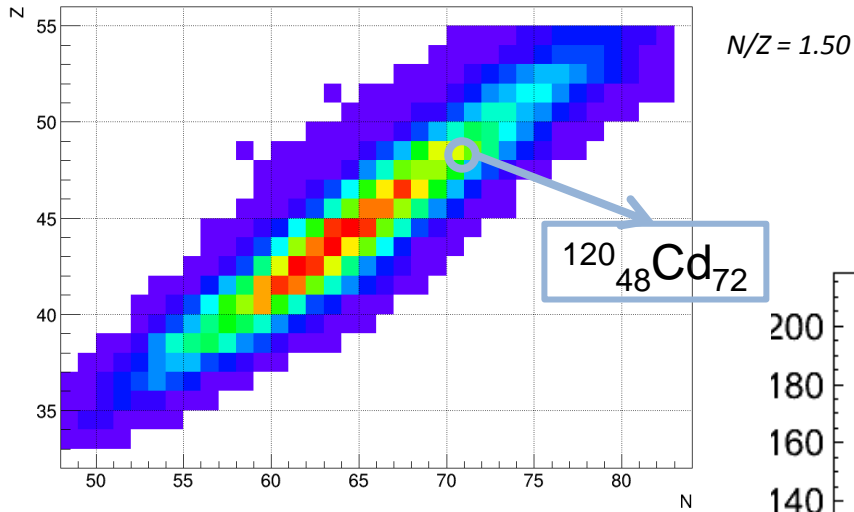
γ rays from isotopically id. fission fragments

$^{238}\text{U}+^9\text{Be}$ @ 6.6 MeV/u

the fission nuclide chart

AGATA+VAMOS commissioning run, December 2014

$^{238}\text{U}+^9\text{Be}$ (6.6 MeV)



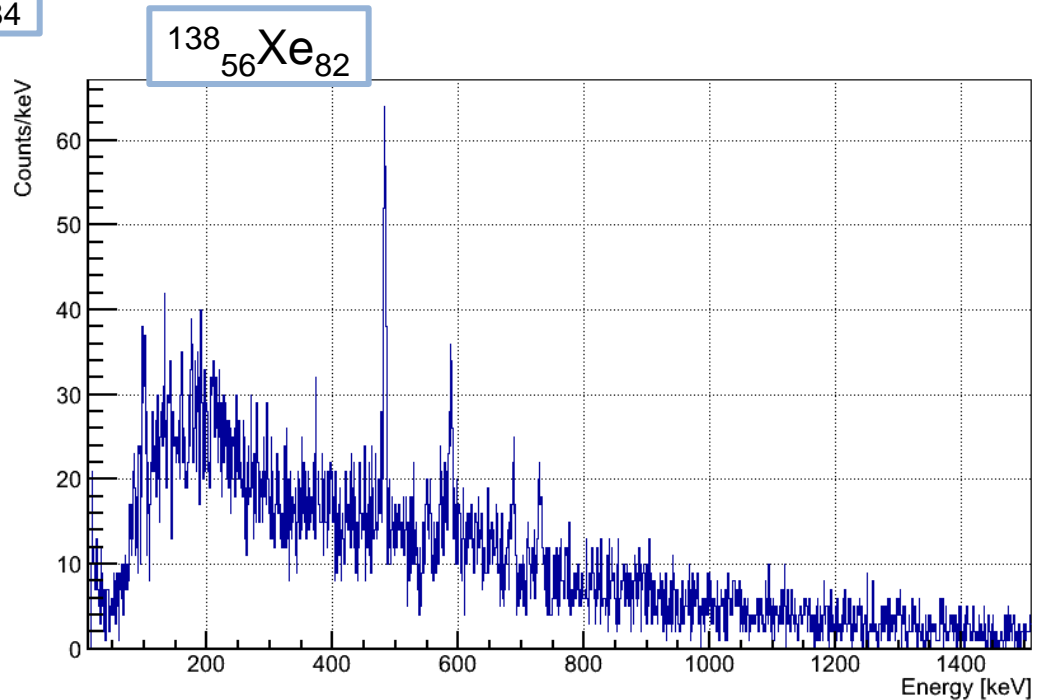
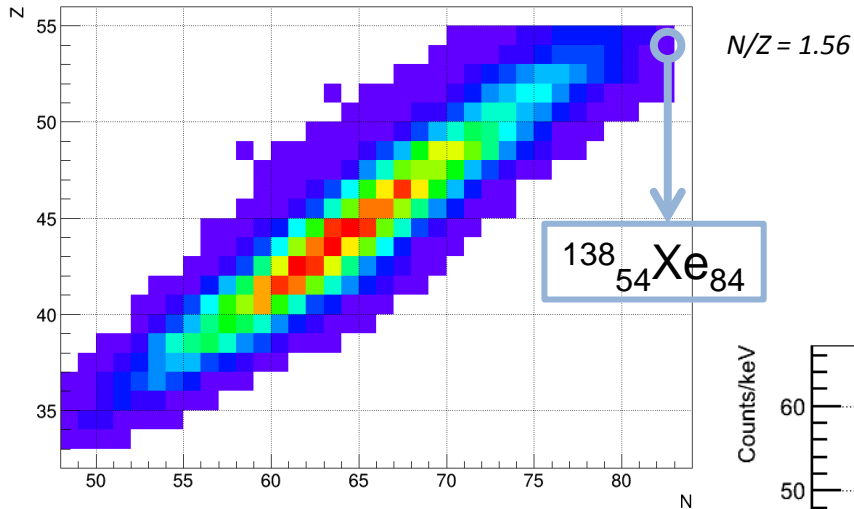
γ rays from isotopically id. fission fragments

$^{238}\text{U}+^9\text{Be}$ @ 6.6 MeV/u

the fission nuclide chart

AGATA+VAMOS commissioning run, December 2014

$^{238}\text{U}+^9\text{Be}$ (6.6 MeV)



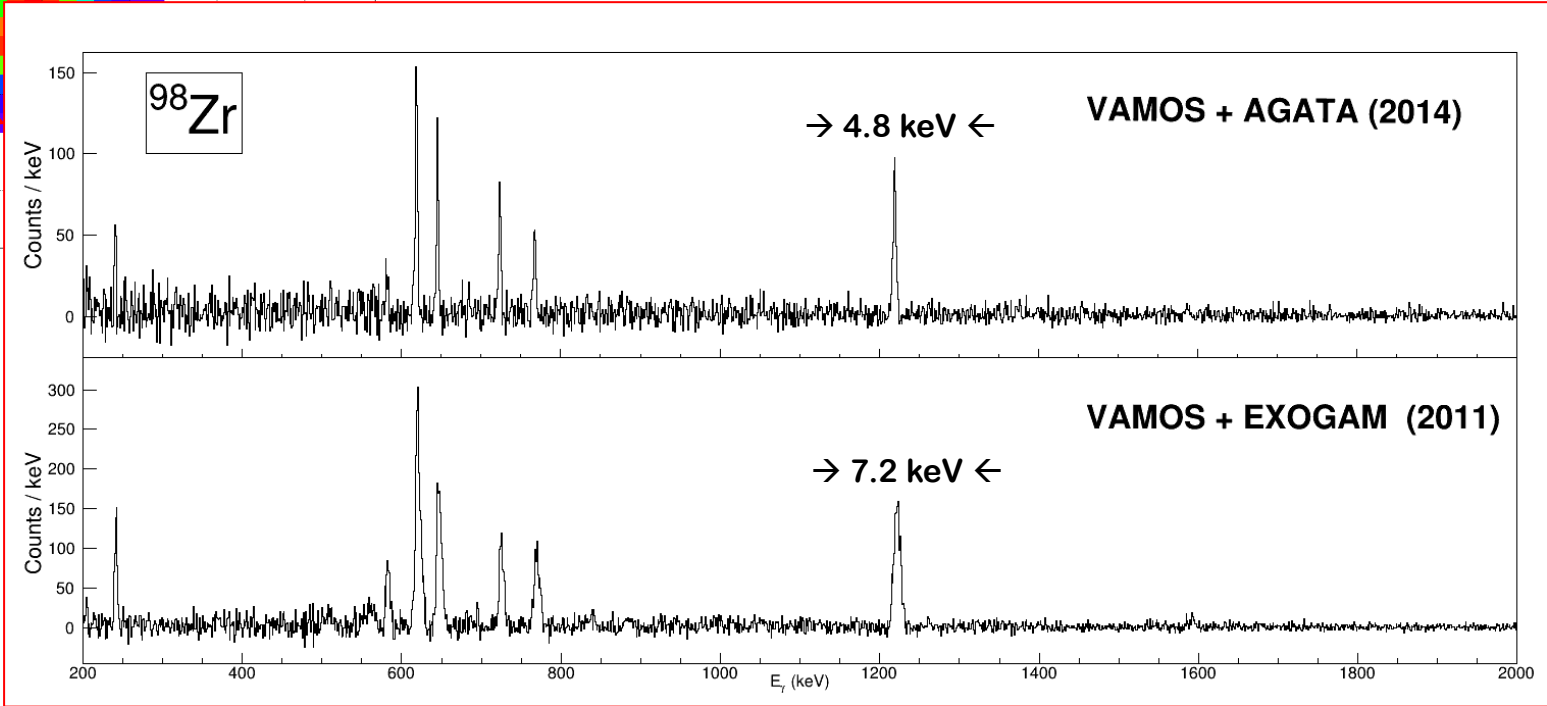
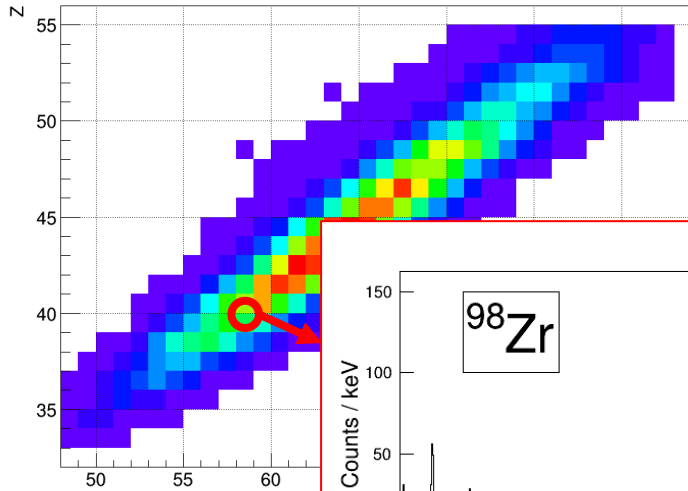
γ rays from isotopically id. fission fragments

$^{238}\text{U}+^9\text{Be}$ @ 6.6 MeV/u

the fission nuclide chart

AGATA+VAMOS commissioning run, December 2014

$^{238}\text{U}+^9\text{Be}$ (6.6 MeV)



Experimental campaign at GANIL AGATA+VAMOS



Study of quadrupole correlations in the $106,108\text{Sn}$ isotopes via lifetime measurements (AGATA+VAMOS+plunger)
J-J. Valiente-Dobon -- June 2015

Lifetime and g factor measurements of short-lived states in the vicinity of ^{208}Pb (AGATA+VAMOS)
G. Georgiev -- May 2015

Test of the $Z=28$ proton and $N=50$ neutron gaps in ^{82}Ge and ^{80}Zn nuclei. Impact on the magicity of ^{78}Ni (AGATA+VAMOS)
G. Duchêne -- May 2015

Neutron monopole drifts near the $N=50$ closed shell towards ^{78}Ni (AGATA+VAMOS+plunger)
D. Verney -- April 2015

Lifetime measurements in the vicinity of ^{68}Ni (AGATA+VAMOS+plunger)
J. Ljungvall -- March 2015

